Yersinia Type III-Secreted Effectors Subvert Caspase-4-dependent Inflammasome Activation in Human Cells

Jenna Zhang[a], Igor E. Brodsky[b,#], and Sunny Shin[a,#]

[a]Department of Microbiology, University of Pennsylvania Perelman School of Medicine, Philadelphia, Pennsylvania 19104

[b]Department of Pathobiology, University of Pennsylvania School of Veterinary Medicine, Philadelphia, Pennsylvania 19104

Running title: *Yersinia* suppresses human inflammasome activation

#Co-corresponding authors: Igor E. Brodsky ibrodsky@vet.upenn.edu and Sunny Shin sunshin@pennmedicine.upenn.edu

Abstract word count: 191

Text word count: 4927

Abstract

Yersinia are gram-negative zoonotic bacteria that use a type three secretion system (T3SS) to inject *Yersinia* outer proteins (Yops) into the host cytosol in order to subvert essential components of innate immune signaling. However, *Yersinia* virulence can elicit activation of immune complexes known as inflammasomes, which lead to inflammatory cell death and cytokine release aimed at containing infection. *Yersinia* activation and evasion of inflammasomes have been characterized in macrophages but remain poorly defined in intestinal epithelial cells (IECs), the primary site of gastrointestinal *Yersinia* infection. In contrast to murine macrophages, we find that in human IECs, *Yersinia pseudotuberculosis* T3SS effectors fully suppress activation of the caspase-4 inflammasome, which senses cytosolic lipopolysaccharide (LPS). The antiphagocytic Yops YopE and YopH, as well as YopK, were entirely responsible for inhibiting inflammasome activation, in part by inhibiting *Yersinia* internalization into IECs. Surprisingly, Yops E, H and K also suppressed inflammasome activation in human macrophages, which, like human IECs, failed to undergo cell death in response to wild-type *Yersinia*. These data suggest species-specific differences underlying inflammasome activation in response to *Yersinia*, and provide insight into the mechanisms of *Yersinia*-mediated inflammasome activation and suppression in human cells.

Importance *Yersinia* are responsible for significant disease burdens in humans, ranging from recurrent disease outbreaks (yersiniosis) to pandemics (*Yersinia pestis* plague). Together with rising antibiotic resistance rates, there is a critical need to better understand *Yersinia* pathogenesis and host immune mechanisms, as this information will aid in developing improved immunomodulatory therapeutics. Intestinal epithelial cells are a critical component of intestinal immunity, yet their inflammasome responses are understudied compared to those of innate immune cells. Furthermore, inflammasome responses in human models are less studied relative to murine models of infection although key innate immune differences exist between mice and humans. Here, we dissect human intestinal epithelial cell and macrophage inflammasome responses to *Yersinia pseudotuberculosis.* Our findings provide fundamental insight into species- and cell-type specific differences in inflammasome responses to *Yersinia.*

Introduction

Innate immune responses are a critical component of host defense and employ pattern recognition receptors (PRRs) to detect pathogen-associated molecular patterns (PAMPs) (1, 2). Specific cytosolic PRRs in the Nucleotide binding domain and Leucine-rich Repeat-containing

protein (NLR) family induce the formation and activation of multimeric immune complexes known as inflammasomes in response to cytosolic PAMPs and distinct stimuli downstream of pathogen virulence-associated activity,(3–5). The NLRP3 inflammasome is activated by a variety of stimuli including potassium efflux downstream of bacterial-induced pore formation (5–9), whereas the NAIP-NLRC4 inflammasome responds to bacterial flagellin and components of bacterial type III secretion systems (T3SS) (10–18). Inflammasomes recruit and activate caspase-1, which in turn processes members of the IL-1 family of cytokines and the pore-forming protein GSDMD into their active forms (19–23). In addition to these canonical inflammasome pathways, a non-canonical caspase-4 inflammasome in humans, and orthologous caspase-11 inflammasome in mice, responds to cytosolic lipopolysaccharide (LPS) during gram-negative bacterial infection to initiate GSDMD pore formation and cytokine release (24–31). Consequently, inflammasome activation leads to release of active IL-1 family cytokines, specifically IL-1β and IL18, and an inflammatory form of cell death known as pyroptosis, that collectively amplify immune signaling and promote anti-bacterial defense (32). In parallel, bacterial infection triggers other programmed cell death pathways, including apoptosis and necroptosis, thereby providing multiple layers of defense against bacterial pathogens (33, 34).

The enteric pathogenic Yersiniae, *Yersinia pseudotuberculosis* and *Y. enterocolitica,* express a conserved T3SS that injects *Yersinia* outer proteins (Yops) into target cells (35). T3SS-injected Yops manipulate host cellular pathways to promote infection, but also activate effector-triggered cell death responses. For example, in murine macrophages, YopJ-mediated suppression of NF-κB signaling induces apoptosis whereas YopE-mediated disruption of cytoskeletal dynamics and hyper-translocation of T3SS components both induce inflammasome activation and subsequent pyroptosis (36–45). Notably, *Yersinia* utilizes two other effectors, YopM and YopK, to evade YopE-triggered pyrin and T3SS-triggered NLRP3 and caspase-11-inflammasome activation respectively and promote infection (42, 43, 45, 46), highlighting competing necessities between host signaling manipulation to facilitate colonization and evasion of ensuing effector-triggered immunity (47).

Inflammasome responses to *Yersinia* have primarily been studied in murine macrophages. However, inflammasomes are expressed in multiple cell types, including intestinal epithelial cells (IECs) (48), which are the first colonization barrier and the primary site of infection of many gastrointestinal pathogens, including *Y. enterocolitica* and *Y. pseudotuberculosis*. In mice, intestinal epithelial-intrinsic NAIP/NLRC4 and caspase-11 inflammasome responses restrict intraepithelial bacterial burdens during infection with enteric

pathogens, including *Salmonella*, *Shigella*, enteropathogenic *Escherichia coli* (EPEC), and *Citrobacter rodentium* (49–55). The NAIP/NLRC4 inflammasome is not present in human IECs, wherein the human homolog of caspase-11, caspase-4, instead plays a critical role in controlling bacterial burdens and driving expulsion of infected cells (49, 56, 57), highlighting species-specific differences as well as cell type-specific differences in inflammasome responses. Importantly, many enteric bacterial pathogens use secreted virulence factors to inhibit IEC death in order to preserve their replicative niche during early infection (58, 59). *Y. enterocolitica* uses two anti-phagocytic Yops, YopE and YopH, to suppress caspase-1 and NLRP3-dependent inflammasome activation in human IECs (60). However, the role of other Yops or other inflammasomes such as the caspase-4 inflammasome, is unknown.

Here, we find that in contrast to mouse macrophages, the *Y. pseudotuberculosis* (*Yptb*) effector YopJ does not induce cell death in human IECs or macrophages. In contrast, during human IEC infection, *Yptb* T3SS-secreted effectors suppress caspase-4 inflammasome and GSDMD-dependent IL-18 release. Surprisingly, NLRP3 was dispensable for inflammasome activation induced by effector-less *Yptb*, as was NAIP/NLRC4, consistent with lack of expression of both inflammasomes in human IECs (56). Both caspase-1 and caspase-8 partially contributed to inflammasome activation, although neither was absolutely required. Instead, inflammasome activation was entirely dependent on caspase-4. Three of the six injected Yops, YopE, YopH, and YopK, collectively suppress activation of caspase-4. Mechanistically, YopE and YopH blockade of bacterial phagocytosis prevented accumulation of intracellular bacteria in IECs and correlated with reduced inflammasome activation. Like in human IECs, we found that YopE, YopH, and YopK also synergistically suppress inflammasome activation in human macrophages, a departure from our current understanding of murine macrophage inflammasome responses to *Yersinia*. These findings demonstrate a key role for disruption of actin-mediated phagocytosis in *Yersinia* evasion of the noncanonical inflammasome in human intestinal epithelial cells and macrophages, thus uncovering important species and cell-type specific differences in inflammasome responses to *Yersinia* infection.

Results

Yptb effectors suppress T3SS-dependent inflammasome activation in human IECs

During infection of murine macrophages, *Yersinia* injects Yops to suppress inflammasome activation (42, 43, 45, 46). However, wild type (WT) *Yersinia* induces rapid cell death (Fig. 1A) and caspase-1 activation due to YopJ-mediated inhibition of NF-κB and MAPK signaling, enabling antibacterial defense despite effector-mediated immune modulation (38, 44,

61, 62). In agreement with previous studies on *Y. enterocolitica* infection of human IECs (60), infection of the human colorectal cell line Caco-2 with WT *Y. pseudotuberculosis* failed to induce release of lactate dehydrogenase (LDH), a marker of dying cells, into the cell supernatant (Fig. 1B), suggesting that human IECs do not undergo cell death in response to WT *Yptb* infection. Consistently, WT *Yptb*-infected cells contained high levels of ATP, indicating that these cells are viable and that WT *Yptb* does not induce cell death in human IECs, in contrast to murine macrophages (Fig. 1A-C).

Lack of cell death in *Yptb*-infected human IECs could be due to a failure to activate programmed cell death pathways, or to suppression of programmed cell death by WT *Yersinia*. During infection of human IECs, *Y. enterocolitica* deploys several injected effectors, specifically YopH and YopE, to suppress inflammasome-dependent cell death (60). To determine if *Yptb* similarly modulates cell death in human IECs using its injected effectors, we infected Caco-2 cells with a strain of *Yptb* lacking all six of its injected effectors *(Δ6 Yptb*) and measured induction of cell death by LDH release and ATP viability assay. Notably, Δ*6 Yptb* triggered significantly higher levels of cell death compared to either mock or WT *Yptb*-infected cells (Fig. 1B and 1C). Further, Δ*6 Yptb*-infected Caco-2 cells robustly cleaved and secreted the inflammasome-dependent cytokine IL-18 compared to mock or WT *Yptb*-infected cells (Fig. 1D and 1E). These data indicate that in the absence of its injected effectors, *Yersinia* triggers inflammasome activation in human IECs, in agreement with prior studies (60). IL-18 release following Δ*6 Yptb* infection was dose-dependent, whereas WT *Yptb* failed to induce IL-18 release across a range of increasing MOIs (Fig. S1A). Consistent with our and others' findings that expression and release of the inflammasome-dependent cytokine IL-1β is very low in human IECs (49, 56, 60), we did not detect IL-1β release during Δ*6 Yptb* infection (Fig. S1B). Inflammasome activation in response to Δ*6 Yptb* infection is T3SS-dependent, as an isogenic *Yptb* strain cured of its virulence plasmid encoding the T3SS did not induce IL-18 release in human IECs (Fig. 1D). Intriguingly, coinfection of Caco-2 cells with Δ*6 Yptb* and increasing doses of *WT Yptb* resulted in a dose-dependent decrease in inflammasome activation (Fig. 1F S1C), indicating that the effectors from WT *Yptb* block inflammasome activation in trans, further supporting a role for *Yersinia*-injected effectors in suppressing inflammasome activation. Collectively, these results indicate that like *Y. enterocolitica*, *Yptb* Yops suppress inflammasome activation in human IECs, a fundamentally distinct outcome from the induction of apoptosis and pyroptosis triggered in murine macrophages during WT *Yersinia* infection (38, 44, 61, 62).

Caspase-4 is required for Δ*6 Yptb*-induced inflammasome activation in human IECs

Caspases play important roles in cleaving and activating inflammasome-dependent cytokines and executing cell death (34). Pretreatment of Caco-2 cells with the pan-caspase inhibitor ZVAD prior to infection with Δ*6 Yptb* completely abrogated IL-18 release and cell death compared to the vehicle control (Fig. 2A, B), indicating that caspases likely mediate inflammasome activation downstream of Δ*6 Yptb* infection in human IECs. As ZVAD broadly inhibits multiple caspases, we next sought to determine which specific caspases are required for Δ*6 Yptb*-induced inflammasome activation in human IECs. Caspase-1 is critical for inflammasome-dependent cytokine release and pyroptosis during bacterial infection (34, 44, 52, 63), and is activated during *Y. enterocolitica* infection of Caco-2 cells (60). To evaluate the role for caspase-1 in inflammasome activation during Δ*6 Yptb* infection, we took parallel genetic and pharmacologic approaches by using *CASP1*$^{-/-}$ Caco-2 cells (56) and the caspase-1 inhibitor YVAD respectively. Δ*6 Yptb* infection of two independent clones of *CASP1*$^{-/-}$ Caco-2 cells resulted in a partial loss of IL-18 release compared to WT Caco-2 cells (Fig. S2A). Additionally, WT Caco-2s pretreated with YVAD exhibited significant but incomplete loss of IL-18 release after Δ*6 Yptb* infection as compared to DMSO vehicle-treated Caco-2 (Fig. S2B), suggesting that caspase-1 contributes to, but is not absolutely required for, Δ*6 Yptb*-induced inflammasome activation. Caspase-8 is activated in response to infection by multiple pathogens, including *Yersinia* (44, 64, 65), and can process caspase-1 substrates such as IL-1β and GSDMD to mediate pyroptosis in the absence of caspase-1 (52, 64, 66). We therefore performed siRNA knockdown of *CASP8* in WT Caco-2, which resulted in 70-80% knockdown of caspase-8 (Fig. S2C). *CASP8* knockdown resulted in a partial reduction in IL-18 release following Δ*6 Yptb* infection (Fig. S2D). We observed a similar reduction when pretreating WT Caco-2 cells with the caspase-8 inhibitor IETD (Fig. S2E), suggesting that like caspase-1, caspase-8 is partially required for inflammasome activation during Δ*6 Yptb* infection. *CASP8* siRNA knockdown in *CASP1*$^{-/-}$ Caco-2 cells also failed to completely abrogate inflammasome activation during Δ*6 Yptb* infection (Fig. S2F, S2G). Together, these results suggest that while both caspase-1 and caspase-8 are contributing to inflammasome activation during Δ*6 Yptb* infection of human IECs, neither is absolutely required and additional caspases likely contribute.

Caspase-4 plays a critical role in human IECs in response to a variety of enteric pathogens (49, 55–57), and its activation triggers both cell death and IL-18 release in intestinal epithelial cells(49). To test whether caspase-4 contributes to inflammasome activation during Δ*6 Yptb* infection, we infected two independent single-cell clones of *CASP4*$^{-/-}$ Caco-2 cells (56) with either WT or Δ*6 Yptb*. As expected, WT *Yptb* infection did not elicit inflammasome activation in either WT or *CASP4*$^{-/-}$ Caco-2 cells. Δ*6 Yptb* infection of WT Caco-2 cells resulted in robust

inflammasome activation, leading to release of cleaved IL-18 and cell death. Notably, CASP4 deficiency in Caco-2 cells abrogated cleavage and release of active IL-18 and cell death in response to Δ*6 Yptb* infection, indicating that caspase-4 is absolutely required for inflammasome activation induced by Δ*6 Yptb* infection in human IECs (Fig. 2C-E). Caspase-5 contributes to *Salmonella*-induced inflammasome activation in Caco-2 cells (56). To test whether caspase-5 also contributes to Δ*6 Yptb*-induced inflammasome activation, we treated WT Caco-2 cells with either a control scramble siRNA or *CASP5* siRNA. Knockdown of *CASP5* resulted in a partial but significant decrease in IL-18 secretion and cell death (Fig. S3B and S3C), suggesting that while caspase-5 plays a contributing role in inflammasome activation, it may not be absolutely required. Collectively, these data indicate that caspase-4 is essential for inflammasome activation in response to Δ*6 Yptb* infection, with caspase-1, -8, and -5 playing contributory roles as well.

GSDMD pore formation downstream of caspase-4 activation is required for Δ*6 Yptb*-induced IL-18 release and cell death in human IECs

Inflammasome activation leads to cleavage of the pore-forming protein GSDMD into its active transmembrane-inserting N-terminal domain, leading to its oligomerization into a large ungated pore (19, 25, 67). Formation of the GSDMD pore in the plasma membrane leads to release of IL-1 family cytokines as well as osmotic cell lysis and death, collectively termed "pyroptosis" (68–71). Caspase-4 cleaves and activates GSDMD via release of its N-terminal domain (25, 72). Notably, Δ*6 Yptb* infection led to robust GSDMD cleavage in WT Caco-2 cells, which was completely absent in *CASP4*$^{-/-}$ Caco-2 cells, indicating that caspase-4 is required for GSDMD cleavage in human IECs in response to *Yersinia* lacking its secreted effectors (Fig. 3A). In contrast, consistent with a lack of observed cell death and IL-18 release, WT *Yptb* infection did not elicit GSDMD cleavage in either WT or two independent *CASP4*$^{-/-}$ clones (Fig. 3A).

To test whether GSDMD is required for inflammasome activation in human IECs during Δ*6 Yptb* infection, we pretreated Caco-2 cells with disulfiram, a chemical inhibitor of GSDMD pore formation (73). Critically, disulfiram treatment completely abrogated IL-18 release and cell death downstream of inflammasome activation in Δ*6 Yptb*-infected cells compared to infected vehicle control treated cells (Fig. 3B and 3C).

The NLRP3 inflammasome can be activated a variety of stimuli during infection, including potassium efflux downstream of caspase-4 and GSDMD activation (5–9). Previous studies of human IEC responses during *Y. enterocolitica* infection identified a critical role for the

NLRP3 inflammasome (60). However, studies of human IECs during *Salmonella* infection found that NLRP3 does not play a role in inflammasome activation, potentially due to very low levels of NLRP3 expression in human IECs as compared to human macrophages (56). Interestingly, WT Caco-2 cells pretreated with a chemical inhibitor of the NLRP3 inflammasome, MCC950, underwent comparable levels of inflammasome activation in response to Δ*6 Yptb* infection as infected vehicle control-treated Caco-2 cells (Fig. S4A). Stimulating Caco-2 cells with LPS and nigericin, a known agonist of the NLRP3 inflammasome, also failed to induce IL-18 release, further suggesting a lack of NLRP3 inflammasome activity in Caco-2 cells. The NAIP/NLRC4 inflammasome, which senses and responds to flagellin and type III secretion system ligands (10–18) (Fig. S4B), and the inflammasome adaptor protein ASC (Fig. S4C) were also dispensable for Δ*6 Yptb*-induced inflammasome activation, consistent with prior findings that expression of these proteins is very low in human IECs (56). Collectively, these results indicate that during Δ*6 Yptb* infection of human IECs, GSDMD cleavage and activation occurs downstream of caspase-4 and is required for IL-18 release and cell death, but the canonical NLRP3 and NAIP/NLRC4 inflammasomes, as well as broadly ASC-dependent inflammasomes, are dispensable.

YopE, YopH, and YopK synergistically suppress inflammasome activation in human cells

Our findings demonstrate that *Yptb* lacking its entire repertoire of injected effectors induce inflammasome activation in human IECs (Fig. 1). In contrast, Caco-2 cells infected with a panel of *Yptb* mutant strains each lacking one of the six Yops failed to elicit IL-18 secretion (Fig. 4A), indicating that loss of any single secreted Yop was insufficient to alleviate inflammasome suppression and that several Yops likely have overlapping functions in suppressing inflammasome activation. Notably, single loss of YopK and YopM failed to induce inflammasome activation (Fig. 4A), despite their roles in suppressing the NLRP3/caspase-11 and pyrin inflammasome respectively in murine macrophages (40, 43, 45, 46). Indeed, *Y. enterocolitica* was previously proposed to regulate NLRP3 inflammasome activation in Caco-2 cells by a combination of YopE and YopH-mediated blockade of “outside-in” integrin signaling (60). Consistently, *Yptb* lacking both YopE and YopH *(*Δ*yopEH Yptb*) elicited significantly elevated IL-18 release downstream of inflammasome activation in Caco-2 cells, indicating that combinatorial loss of both YopE and YopH was sufficient to alleviate inflammasome suppression in human IECs (Fig. 4B). Nonetheless, IL-18 levels during Δ*yopEH Yptb* infection were still significantly lower than IL-18 levels released during Δ*6 Yptb* infection (Fig. 4B),

suggesting that additional Yops contribute to inflammasome suppression during *Yersinia* infection of human IECs.

YopK is a translocated effector that negatively regulates the translocation of other effector proteins and T3SS components (42, 43, 45). In murine macrophages, YopK suppresses inflammasome activation, whereas YopE and YopH do not contribute to inflammasome suppression (42, 43, 45). Given that deletion of *yopK* alone failed to elicit IL-18 release in human IECs (60) (Fig. 4A), we considered that YopK modulates inflammasome activation in human IECs in a manner that is masked by YopE and YopH, perhaps because these effectors are hypertranslocated in a *yopK* mutant. We therefore infected Caco-2 cells with a combined mutant *Yptb* strain lacking *yopE*, *yopH* and *yopK (*Δ*yopEHK Yptb*) and assayed for IL-18 release downstream of inflammasome activation. Notably, IL-18 release during Δ*yopEHK Yptb* infection was substantially elevated compared to Δ*yopEH Yptb,* and fully recapitulated levels of IL-18 observed during Δ*6 Yptb* infection (Fig. 4B). These data indicate that YopE, YopH and YopK function together to suppress inflammasome activation during infection. Importantly, individual loss of YopK, dual loss of YopK and YopE *(*Δ*yopEK*) or dual loss of YopK and YopH *(*Δ*yopHK*) all failed to induce inflammasome activation. Only in a *yopEH* mutant background did additional deletion of YopK lead to an increase in IL-18 release (Fig. 4B). Further, as with Δ*6 Yptb* infection, Δ*yopEHK*-induced inflammasome activation was fully dependent on the caspase-4 inflammasome (Fig. 4C, 4D). Taken together, these data suggest that YopE, YopH, and YopK act to inhibit components of a shared inflammasome-activating pathway, a departure from the murine macrophage literature where YopK and YopM but not YopE or H, suppress inflammasome activation (42, 43, 45, 46)

Fundamental differences exist between human and murine macrophage inflammasome responses to enteric pathogens such as *Salmonella* Typhimurium (74–76). As such, we hypothesized that human macrophage responses to *Yptb* infection may similarly diverge from those of murine macrophages. Infection of the human monocytic THP-1 cell line revealed that Δ*yopEH* and Δ*yopEHK* infection induced IL-1β and pyroptosis downstream of inflammasome activation (Fig. 4E and 4F). As was the case during infection of human IECs, Δ*yopEHK* infection triggered higher levels of inflammasome activation than Δ*yopEH* infection in THP-1 cells (Fig. 4E and 4F). These data indicate that human macrophages behave similarly to human IECs, with Yops E and H functioning together with YopK to suppress inflammasome activation. Intriguingly, and in marked contrast to established findings in murine macrophages, WT *Yptb* also did not induce cell death in human macrophages, implying that WT *Yptb* effectively suppresses cell death in human IECs and macrophages (Fig. 4F vs 1A). These data suggest that species-

specific differences exist in the response to the activities of *Yersinia* effector proteins between human and murine cells addition to cell-type specific differences. Overall, these results reveal a role for Yops E, H and K in synergistically suppressing inflammasome activation in human IECs and macrophages.

YopE and YopH inhibit caspase-4-dependent inflammasome activation by blocking actin-dependent bacterial phagocytosis in human IECs

During *Y. enterocolitica* infection of human IECs, YopE and YopH suppress inflammasome activation by disrupting signaling downstream of *Yersinia* invasin binding to host β1-integrin receptor (60). Invasin-β1-integrin interactions initiate host cytoskeletal rearrangements to facilitate bacterial internalization (77–80), and YopE and YopH disruption of focal adhesion complexes and actin filamentation consequently inhibits *Yersinia* uptake into host cells (80–87). Notably, consistent with both Δ*6* and Δ*yopEHK Yptb* infection, we found that caspase-4 was absolutely required for inflammasome activation induced by Δ*yopEH Yptb* infection (Fig. 5A and 5B). Considering YopE and YopH's known role in inhibiting bacterial internalization, we hypothesized that YopE and YopH suppression of inflammasome activation in human IECs is linked to their antiphagocytic activity, which would limit bacterial internalization, subsequent cytosolic delivery of LPS, and caspase-4 inflammasome activation. We therefore assessed *Yptb* internalization into human IECs by measuring intracellular bacterial burdens at 2 hours post-infection. As expected, intracellular bacterial burdens were lowest in WT *Yptb*-infected cells, while Δ*yopEH*-infected cells had significantly elevated levels of intracellular bacteria, as did Δ*yopEHK* and Δ*6*-infected cells (Fig. 5C and Fig. S5A). Δ*yopEHK* and Δ*6*-infected cells had comparable levels of intracellular bacteria to Δ*yopEH*-infected cells at 2 hpi, indicating that YopE and YopH regulate phagocytosis inhibition in human IECs, while YopK limits inflammasome activation through a mechanism distinct from phagocytosis inhibition. To corroborate our bacteriologic observation that YopE and YopH suppress IEC internalization of *Yersinia*, we performed microscopic analysis on Caco-2 cells infected with GFP-expressing WT, Δ*yopEH*, or Δ*6 Yptb*. In agreement with our CFU data, Δ*yopEH Yptb*-infected cells had a significantly higher levels of intracellular bacteria (i.e. GFP only bacteria) than WT *Yptb*-infected cells, and levels of intracellular bacteria in Δ*yopEH* and Δ*6 Yptb* infected cells were similar (Fig. 5D, 5E, S5B). As YopE and YopH block bacterial uptake via disruption of actin filamentation, we thus asked whether pharmacological inhibition of the actin cytoskeleton would complement inhibition of bacterial uptake during Δ*yopEH Yptb* infection of human IECs. Indeed, pretreating Caco-2 cells with cytochalasin D, an inhibitor of actin polymerization, reduced levels of

intracellular bacteria following Δ*yopEH* infection to that of WT *Yptb* infection (Fig. 5F and S5C). Furthermore, cytochalasin D treatment completely abrogated inflammasome activation during Δ*yopEH* and Δ*6 Yptb* infection (Fig. 5G), suggesting that inhibition of phagocytosis restored inflammasome suppression in Δ*yopEH Yptb*-infected human IECs. Collectively, these results point to a link between YopE and YopH-mediated inhibition of phagocytosis and inflammasome activation, offering a potential mechanism by which YopE and YopH mediate inflammasome evasion by *Yptb* in human IECs.

Discussion

In this study, we demonstrate that *Y. pseudotuberculosis* injected effectors suppress caspase-4-dependent inflammasome activation, GSDMD-mediated cell death, and IL-18 release in human intestinal epithelial cells (IECs) (Fig. 1-3, S1). Caspase-1, caspase-8 and caspase-5 partially contribute, but none individually or in combination were required for this response (Fig. S2, S3). Consistent with their low levels of expression in IECs, the NAIP/NLRC4 and NLRP3 inflammasomes did not contribute to this inflammasome activation, nor did the adaptor protein ASC, which is utilized by multiple inflammasomes to mediate caspase recruitment (Fig. S4). Collectively these data imply that canonical inflammasomes are not activated during *Yptb* infection of IECs. Rather, we report here that YopE, YopH, and YopK act in concert to suppress caspase-4 inflammasome activation in human IECs.

While loss of YopK alone had no effect on inflammasome suppression, YopK deletion in the absence of YopE and YopH phenocopied Δ*6 Yptb* infection and resulted in maximum inflammasome activation, suggesting that YopK suppresses a component of an inflammasome-activating pathway masked by the activity of YopE and YopH (Fig. 4). Consistent with prior findings in *Y. enterocolitica* infection (60), we found that WT *Yptb* does not induce YopJ-dependent cell death in human IECs, in contrast to *Yersinia* interactions reported in murine macrophages. Surprisingly, during infection of human macrophages, WT *Yptb* also fails to induce cell death and deploys YopE, YopH and YopK to synergistically suppress inflammasome activation (Fig. 4). Finally, we demonstrate, in agreement with previous findings (80–84), that YopE and YopH block bacterial internalization into IECs. YopE and YopH are known to inhibit cytoskeletal dynamics, and we found that chemical inhibition of actin polymerization mimicked YopE and H by ablating both inflammasome activation and bacterial internalization (Fig. 5 and S5).

Previous studies found that *Y. enterocolitica* infection of murine macrophages and human IECs activates the NLRP3 inflammasome (45, 60). Surprisingly, we found that NLRP3

was dispensable for inflammasome activation during *Y. pseudotuberculosis* infection of Caco-2 cells (Fig. S4A). Furthermore, known activators of NLRP3 failed to induce inflammasome activation in Caco-2 cells (56) (Fig. S4A). Consistently, NLRP3 expression is very low in Caco-2 cells and human intestinal enteroids and colonoids, and NLRP3 is dispensable for inflammasome activation during *Salmonella* infection of human IECs (56). However, human patient mutations in NLRP3 have been found to be associated with development of Crohn's disease, suggesting that there may be a gastrointestinal role for this inflammasome in humans despite its low expression (88). It is possible that differences in cell culture conditions or *Y. enterocolitica* and *Y. pseudotuberculosis* infection properties may account for the differential role of NLRP3 during respective infections of human IECs, and that under certain conditions, low levels of NLRP3 are able to respond and execute inflammasome activation in human IECs.

We found instead that caspase-4 was absolutely required for inflammasome activation during *Y. pseudotuberculosis* infection of human IECs (Fig. 2, 4C-D, 5A-B). Caspase-4 is more highly expressed in human IECs than other inflammasome components (56), and a broad range of intracellular enteric pathogens engage or inhibit caspase-4/11 in human and murine IECs, respectively (49–59). In myeloid cells, activated caspase-4/11 directly executes cell death, but requires NLRP3 and caspase-1 for downstream IL-18 maturation and secretion (24). However, it has been reported that in IECs, caspase-1 is dispensable for IL-18 release, whereas caspase-4 is absolutely required (49, 55, 57, 89). Indeed, we found that caspase-1 is not required for IL-18 release or cell death during *Yptb* infection of human IECs, although it plays a partial role (Fig. S2A and S2B). We similarly found a partial role for caspase-8 in cell death (Fig. S2D and S2E). Caspase-8 and caspase-1 can be recruited to the same inflammasome complexes and can have redundant or compensatory roles (52, 63). Moreover, caspase-8 cleaves and activates caspase-1 in response to YopJ-dependent NF-κB blockade during *Yersinia* infection in murine macrophages (44). However, we found that YopJ did not impact inflammasome activation during *Y. pseudotuberculosis* infection of Caco-2 cells, indicating that fundamentally distinct pathways mediate *Yptb*-induced cell death in IECs. Whether caspase-8 and capase-1 are activated downstream of caspase-4 or whether they are acting in a parallel pathway during *Yersinia* infection of human IECs is still an open question. Simultaneous knockdown of caspase-1 and caspase-8 still allowed for release of IL-18 during Δ*6 Yptb* infection (Fig. S2F), suggesting that caspase-1 and caspase-8 are unlikely to play overlapping roles and instead potentially act sequentially. These results also raise the possibility that there is a role for other caspases, such as caspase-10, in inflammasome activation in human IECs.

Our findings that YopE and YopH block bacterial internalization into human IECs are consistent with known functions of YopE and H (80–84), and demonstrate that in the absence of YopE and YopH, bacterial uptake and inflammasome activation are able to occur (Fig. 5 and S4). We hypothesize that blocking uptake of the bacteria into the host cell enables *Yptb* to limit delivery of bacterial LPS into the host cell, thereby limiting the activation of the noncanonical inflammasome. These findings suggest a potential mechanism by which YopE and YopH enable *Yptb* to evade caspase-4 inflammasome activation during infection. Intriguingly these results are a departure from the paradigm of YopE-dependent activation of the pyrin inflammasome via disruption of cytoskeletal dynamics in murine macrophages (40, 46). In the murine macrophage system, this activation is suppressed by YopM, yet we found that during human IEC infection YopM was dispensable for inflammasome suppression even in the presence of YopE (Fig. 4A).

A previous study proposed that during *Y. entercolitica* infection of IECs, YopE and YopH suppress inflammasome activation by blocking a critical priming “first signal” downstream of integrin signaling that upregulates IL-18 transcript levels (60). The downstream signaling elements of integrin binding are crucial for initiation of phagocytosis as well, and thus it is possible that YopE and YopH disruption of FAK and RhoGTPase signaling contributes to inflammasome suppression both by limiting intracellular LPS and inhibition of the “first signal”. After being internalized, *Yersinia* enters a membrane-enclosed vacuole that it remodels to facilitate intracellular survival (90–92). In murine macrophages, YopK prevents LPS-mediated noncanonical inflammasome activation by limiting hypertranslocation of T3SS components YopB and D, thus maintaining vacuolar integrity and preventing destabilization of the *Yersinia*-containing vacuole (42, 43). Critically, in human IECs, we found that YopK contributes to caspase-4-inflammasome suppression downstream of YopE and YopH and that inflammasome activation in the absence of Yops E, H and K is T3SS-dependent (Fig. 4B and 1D). It is possible that in the absence of YopE, YopH and YopK, *Yersinia* is more readily taken up into IECs downstream of integrin binding, and *Yersinia*-derived LPS is somehow exposed to the cytosol from within its vacuole, perhaps due to T3SS activity. Further studies are needed to determine whether *Yersinia* LPS is exposed to the cytosol and binds to caspase-4, as well as the precise contribution of YopE, YopH and YopK to inhibition of this process in human IECs.

The synergistic blockade of caspase-4 inflammasome activation by YopE, YopH, and YopK, as well as absence of YopJ-induced cell death, in both human IECs and THP1 macrophages represents a fundamentally distinct model from the murine macrophage response, suggesting that *Yersinia* infection may trigger both cell type-specific and species-specific inflammasome responses. Varying cellular properties and general organ systems needs

may underly these differential responses. For example, as components of a physical as well as innate immune barrier, it may be advantageous for IECs to modulate and execute tightly coordinated responses downstream of virulence detection in order to avoid disruption to the monolayer that bacteria can use as access points (84, 93). Whether inflammasome activation induces changes in the intestinal epithelium during *Yersinia* infection is unknown and would be worth exploring in the future. Furthermore, unlike macrophages, IECs are not phagocytic and as such, cytosolic LPS may be a more specific indicator of virulence activity in IECs, leading to a stronger reliance on caspase-4-mediated responses. Surprisingly, during human macrophage infection *Yptb* also deployed Yops E, H and K to suppress inflammasome activation and failed to induce YopJ-dependent cell death, suggesting that certain inflammasome dynamics may be shared between multiple cell types within a given species and differ broadly between disparate species like mice and humans. Further studies comparing inflammasome responses between murine and human IECs and murine and human macrophages will provide important insight into cell type-specific and species-specific differences in inflammasome pathways.

Overall, our data demonstrate that *Yersinia* employs three injected Yops, YopE, YopH, and YopK, to inhibit caspase-4 and GSDMD-dependent inflammasome activation in human IECs. These Yops also inhibit inflammasome activation in human macrophages, in a manner distinct from what has been previously observed in murine macrophages. These findings lend further support to the critical role for the caspase-4 inflammasome in human IECs during host defense against enteric pathogens and provide new insight into innate immune interactions between *Yersinia* and a critical component of intestinal immunity. Moreover, it highlights how inflammasome responses can vary between different cell types and between mice and humans, which provides crucial insight into how inflammasome responses contribute to human health and disease.

Materials and Methods

Bacterial strains and growth conditions

Yersinia strains are described in Table S1 in the supplemental material. Δ*yopEHK*, Δ*yopEK*, and Δ*yopHK* were generated by introducing a frameshift mutation of the *yopK* open reading frame into the Δ*yopEH*, Δ*yopE* and Δ*yopH* backgrounds respectively using a plasmid provided by Dr. James Bliska and an allelic exchange method (94). Δ*yopM* was generated by introducing an unmarked deletion of the *yopM* open reading frame into IP2666 using a plasmid provided by Dr. James Bliska and the same allelic exchange method. Yersiniae were cultured overnight at 26°C with aeration in 2x yeast extract-tryptone (YT) broth. To induce T3SS expression, in the morning, the bacteria were diluted into fresh 2xYT containing 20 mM sodium oxalate and 20 mM $MgCl_2$. Bacteria were grown with aeration for 1 hour at 26°C followed by 2 hour at 37°C prior to infection. All cultures were pelleted at 6000 x *g* for 3 min and resuspended in phosphate-buffered saline (PBS). Cells were infected at an MOI of 60 unless otherwise indicated, centrifuged at 290 x *g* for 10 min and incubated at 37°C. At 1 hour post-infection, cells were treated with 20 ng/ml or 100 ng/ml of gentamicin for 6 hour or 2 hour time points respectively. Infections proceeded at 37°C for the indicated length of time for each experiment. In all experiments control cells were mock infected with PBS.

Cell culture of cell lines

Caco-2 cells (HTB-27; American Type Culture Collection) were maintained in Dulbecco's modified Eagle's medium (DMEM) supplemented with 10% (vol/vol) heat-inactivated fetal bovine serum (FBS), 100 IU/mL penicillin and 100 μg/mL streptomycin. THP-1 cells (TIB-202; American Type Culture Collection) were maintained in RPMI supplemented with 10% (vol/vol) heat-inactivated fetal bovine serum (FBS), 0.05 nM β-mercaptoethanol, 100 IU/mL penicillin and 100 μg/mL streptomycin. All cells were grown at 37°C in a humidified incubator with 5% CO_2. One day prior to infection, Caco-2 cells were incubated with 0.25% trypsin-EDTA (Gibco) diluted 1:1 with 1 x PBS at 37°C for 15 min to dissociate cells. Trypsin was neutralized with serum-containing medium. Cells were replated in medium without antibiotics in a 24-well plate at a density of 3 x 10^5 cells/well. Two days prior to infection, THP-1 cells were replated in medium without antibiotics in a 48-well plate at a density of 2 x 10^5 cells/well and incubated with phorbol 12-myristate 13-acetate (PMA) for 24 hours to allow differentiation into macrophages.

Macrophages were primed with 100 ng/mL Pam3CSK4 (Invivogen) for 16 hours prior to bacterial infections.

ELISAs

Supernatants harvested from infected cells were assayed using enzyme-linked immunosorbent assay (ELISA) kits for human IL-18 (R&D Systems) and IL-1β (BD Biosciences).

LDH cytotoxicity assays

Supernatants harvested from infected cells were assayed for cytotoxicity by measuring loss of cellular membrane integrity via lactate dehydrogenase (LDH) assay. LDH release was quantified using an LDH Cytotoxicity Detection Kit (Clontech) according to the manufacturer's instructions and normalized to mock-infected (min cytotoxicity) and 2% triton-treated cells (max cytotoxicity)

Cell viability assay

Viability of infected cells was assessed using the CellTiter-Glo 2.0 Assay Kit (CTG2.0; Promega) according to manufacturer's instructions. Caco-2 cells were seeded in 96-well flat bottom white polystyrene TC-treated microplates (Corning) at a density of 7.5 x 10^4 cells/well in medium without antibiotics. Cells were infected at an MOI of 60 and treated with 20 ng/mL gentamicin 1hpi. After 6 hours, cells were treated with CTG2.0 reagent mix and incubated in the dark at 37°C for 30 min. Luminescence was read on a luminometer and values normalized to cells treated with 1% TritonX-100 (min cell viability) and mock-transfected cells (max cell viability)

Immunoblot analysis

Cells were replated and infected on serum-free medium to collect supernatant samples. Supernatant samples were centrifuged at 200 x *g* to pellet any cell debris and treated with trichloroacetic acid (TCA) (25 μL TCA per 500 μL supernatant) overnight at 4°C. The following day, TCA-treated samples were centrifuged at max speed (15,871 x *g*) for 15 min at 4°C and washed with ice-cold acetone. TCA-precipitated supernatant samples and cell lysates were resuspended in 1 x SDS-PAGE sample buffer and boiled for 5 min. Samples were separated by SDS-PAGE on a 12% (vol/vol) acrylamide gel and transferred to polyvinylidene difluoride (PVDF) Immobilon-P membranes (Millipore). Primary antibodies specific for human IL-18 (MLB International PM014), β-actin (4967L; Cell Signaling) and GSDMD (G7422 Sigma-Aldrich) and

519 horseradish peroxidase (HRP)-conjugated secondary antibody anti-rabbit IgG (7074S; Cell
520 Signaling) were used. Enhanced chemiluminescence (ECL) Western blotting substrate or
521 SuperSignal West Femto (Pierce Thermo Scientific) HRP substrate were used for detection.
522
523 **Inhibitor experiments**
524 Cells were treated 1 h prior to infection at the indicated concentrations of the following inhibitors:
525 10 μM MCC950 (Sigma-Aldrich; PZ0280), 20 μM pan-caspase inhibitor Z-VAD(Ome)-FMK (SM
526 Biochemicals; SMFMK001), 20 μM caspase-1 inhibitor Ac-YVAD-cmk (Sigma-Aldrich;
527 SML0429), and 30 μM disulfiram (Sigma).
528
529 **siRNA-mediated gene knockdown**
530 *CASP5* (S2417), *CASP8* (S2427), and two Silencer Select negative-control siRNAs (Silencer
531 Select negative control no. 1 and no. 2 siRNA) were purchased from Ambion (Life
532 Technologies). Three days before infection, 30 nM siRNA was transfected into Caco-2 cells
533 using Lipofectamine RNAiMAX transfection reagent (Thermo Fisher Scientific) following the
534 manufacturer's protocol.
535
536 **Quantitative RT-PCR analysis**
537 RNA was isolated using the RNeasy Plus Mini Kit (Qiagen) following the manufacturer's
538 instructions. Cells were lysed in 350 μL RLT buffer with β-mercaptoethanol and centrifuged
539 through a QIAshredder spin column (Qiagen). cDNA was synthesized from isolated RNA using
540 SuperScript II Reverse Transcriptase (Invitrogen) following the manufacturer's instructions.
541 Quantitative PCR was conducted with the CFX96 real-time system from Bio-Rad using the
542 SsoFast EvaGreen Supermix with Low ROX (Bio-Rad). For analysis, mRNA levels of siRNA-
543 treated cells were normalized to housekeeping gene *HPRT* and control siRNA-treated cells
544 using the $2^{-\Delta\Delta CT}$ (cycle threshold) method to calculate knockdown efficiency (95). The following
545 primers were used:
546 *CASP5* forward: TTCAACACCACATAACGTGTCC
547 *CASP5* reverse: GTCAAGGTTGCTCGTTCTATGG
548 *CASP8* forward: GTTGTGTGGGGTAATGACAATCT
549 *Casp8* reverse: TCAAAGGTCGTGGTCAAAGCC
550 *HPRT* forward: CCTGGCGTCGTGATTAGTGAT
551 *HPRT* reverse: AGACGTTCAGTCCTGTCCATAA
552

Bacterial uptake enumeration with colony forming units (CFUs)

Cells were infected with indicated strains of *Yersinia* at an MOI of 20. 1 hpi, cells were treated with 100 μg/mL of gentamicin to kill extracellular bacteria. 2 hpi the supernatants were aspirated and cells were lysed with PBS containing 0.5% Triton to collect intracellular bacteria. Harvested bacteria were serially diluted in PBS and plated on LB agar plates containing 2 μg/mL Irgasan. Plates were incubated at 28°C for two days and CFUIs were counted.

Fluorescence microscopy of intracellular *Yersinia*

One day before infection 2 x 10^5 cells/well were plated on glass coverslips in a 24-well plate. Cells were infected with indicated strains of *Yersinia* constitutively expressing GFP at an MOI of 20. At 2hpi, cells were washed 2 times with PBS, fixed with 4% paraformaldehyde for 10 min at 37°C and stored overnight at 4°C in PBS. The following day, cells were blocked for 30 min at room temperature in blocking solution containing 1% BSA in PBS and incubated for 1 h at room temperature in blocking solution with the polyclonal anti-*Yersinia* antibody SB349 diluted 1:1000 (kindly provided by Dr. James Bliska) (82). AF594-conjugated goat anti-Rabbit IgG antibody (A-11012 Thermo Fisher Scientific) was diluted 1:500 in blocking solution was added to cells and incubated for 45 min at room temperature. Cells were mounted on glass slides with DAPI mounting medium (Sigma Fluoroshield). Coverslips were imaged on an inverted fluorescence microscope (IX81; Olympus) and images were collected using a high-resolution charge-coupled-devise camera (FAST1394; QImaging) at a magnification of 60x. Images were analyzed and presented using SlideBook (version 5.0) software (Intelligent Imaging Innovations, Inc.). Average intracellular bacteria/cell and %intracellular bacteria were scored by counting 20 captures per coverslip across triplicate coverslips.

Statistical analysis

Prism 9.4.1 (GraphPad Software) was utilized for the graphing of data and all statistical analyses. Statistical significance for experiments were determined using the appropriate test and are indicated in each figure legend. Differences were considered statistically significant if the p value was <0.05.

Data availability

All data are included in the manuscript and supplemental material. Bacterial strains available upon request

Acknowledgments

We thank members of the Shin and Brodsky laboratories for helpful scientific discussions. We thank Dr. James Bliska for generously providing plasmids and Yop mutant strains.

This work is supported by NIH/NIAID grants AI151476, AI118861, AI123243 (S.S.), AI128630, AI163596, and AI139102 (I.E.B). S.S. and I.E.B. are both recipients of the Burroughs-Welcome Fund Investigators in the Pathogenesis of Infectious Disease Award. J.Z. is a recipient of the NIH/NIAID Microbial Pathogenesis and Genomics training grant 5T32AI141393-03.

Figure 1: *Yptb* T3SS-injected effectors suppress inflammasome activation in human IECs. BMDMs (A) or Caco-2 cells (B-F) were infected with PBS (Mock or MOI 0), WT *Yptb*, or *Δ6 Yptb*. (A, B) Cell death was measured as percent cytotoxicity normalized to cells treated with 2% Triton at 6hpi. (C) Cell death was measured as percent viability normalized to mock-infected cells at 6hpi. (D) Release of IL-18 into the supernatant was measured by ELISA at 6hpi. (E) Lysates and supernatants collected 6hpi were immunoblotted for IL-18 and β-actin. (F) Release of IL-1i into the supernatant was measured by ELISA at 6hpi. ns — not significant, ** $p < 0.01$, *** $p < 0.001$, **** $p < 0.0001$ by Welch's t test (A-C) or by one-way ANOVA (D, F). Error bars represent the standard deviation of triplicate wells and are representative of two or three independent experiments.

Figure 2: caspase-4 is required for *Δ6 Yptb*-induced inflammasome activation in human IECs. (A, B) One hour prior to infection, WT Caco-2 cells were treated with 20 uM ZVAD or DMSO as a vehicle control. Cells were then infected with PBS (Mock), WT *Yptb* or *Δ6 Yptb*. At 6hpi (A) release of IL18 into the supernatant was measured by ELISA and (B) cell death was measured as percent cytotoxicity normalized to cells treated with 2% triton. (C-E) WT or two independent single cell clones of *CASP4*-/- Caco-2 cells were infected with PBS (Mock), WT *Yptb* or *Δ6 Yptb*. (C) Release of IL-18 into the supernatant was measured by ELISA at 6hpi. (D) Lysates and supernatants collected 6hpi were immunoblotted for IL-18 and β-actin. (E) Cell death was measured at 6hpi as percent cytotoxicity normalized to cells treated with 2% triton. ** $p < 0.01$, *** $p < 0.001$, **** $p < 0.0001$ by two-way ANOVA. Error bars represent the standard deviation of triplicate wells and are representative of two or three independent experiments.

Figure 3: GSDMD pore formation downstream of caspase-4 activation is required for *Δ6 Yptb*-induced inflammasome activation in human IECs. (A) WT or two independent single cell clones of *CASP4*-/- Caco-2 cells were infected with PBS (Mock), WT *Yptb* or *Δ6 Yptb*. Lysates and supernatants were collected at 6hpi and immunoblotted for GSDMD and β-actin. (B, C) One hour prior to infection, WT Caco-2 cells were treated with 30 uM disulfiram or DMSO as a vehicle control. Cells were then infected with PBS (Mock), WT *Yptb* or *Δ6 Yptb*. (B) Release of IL-18 into the supernatant and (C) percent cytotoxicity normalized to cells treated with 2% triton were measured at 6hpi. **** $p < 0.0001$ by two-way ANOVA. Error bars represent the standard deviation of triplicate wells and are representative of three independent experiments.

Figure 4: YopE, YopH, and YopK synergistically suppress inflammasome activation in human cells. (A, B) WT Caco-2 cells were infected with PBS (Mock) or indicated strain of *Yptb*. Release of IL-18 into the supernatant was measured at 6hpi. (C, D) WT or two independent single cell clones of *CASP4*-/- Caco-2 cells were infected with PBS (Mock) or the indicated strain of *Yptb*. (C) Release of IL-18 into the supernatant and (D) percent cytotoxicity normalized to cells treated with 2% triton were measured at 6hpi. (E, F) WT THP-1 monocyte-derived macrophages were primed with 100 ng/ml Pam2CSK4 for 16 hours. Cells were infected with PBS (Mock) of the indicated strain of *Yptb*. (E) Release of IL-1β into the supernatant and (F) percent cytotoxicity normalized to cells treated with 2% triton were measured at 6hpi. * $p < 0.05$, *** $p < 0.001$, **** $p < 0.0001$ by one-way ANOVA (A, B, E, F) or two-way ANOVA (C, D). Error bars represent the standard deviation of triplicate wells and are representative of two or three independent experiments.

Figure 5: YopE and YopH inhibit caspase-4-dependent inflammasome activation and actin-dependent bacterial phagocytosis in human IECs. (A, B) WT or two independent single cell clones of *CASP4*-/- Caco-2 cells were infected with PBS (Mock) or the indicated strain of *Yptb*. (A) Release of IL-18 into the supernatant and (B) percent cytotoxicity normalized to cells treated

with 2% triton were measured at 6hpi. (C) WT Caco-2 cells were infected with the indicated strain of *Yptb* at an MOI=20 and lysed at 2 hpi. Bacteria were plated on *Yersinia*-selective agar to calculate CFUs. (D, E) WT Caco-2 cells were seeded on glass coverslips and infected with indicated strain of *Yptb* expressing GFP at an MOI=20. Cells were fixed at 2hpi and stained for extracellular *Yersinia* (Red) and DAPI to label DNA (blue). (D) Representative images are shown. Scale bar represents 10 μm. (E) Proportion of total bacteria that was intracellular (green only) was scored by fluorescence microscopy. Bars represent standard deviation of triplicate coverslips with 20 fields scored per coverslip. (F, G) One hour prior to infection, WT Caco-2 cells were treated with 10 uM cytochalasin D or DMSO as a vehicle control. Cells were then infected with PBS (Mock) or indicated strain of *Yptb*. (F) Cells were lysed at 2hpi and bacteria were plated on *Yersinia*-selective agar to calculate CFUs. (G) Release of IL-18 into the supernatant was measured at 6hpi. * $p < 0.05$, ** $p < 0.01$, **** $p < 0.0001$ by two-way ANOVA (A, B, F, G) or one-way ANOVA (C, E). Error bars represent the standard deviation of triplicate wells and are representative of two or three independent experiments

Table s1: *Yersinia* strains used in this study

Strain name	Relevant characteristics	Reference or Source
IP2666 (WT *Yptb*)	Wild-type, pYV$^+$, naturally *yopT*$^-$	(94)
Δ6 Yptb	*yopEHJMKO*$^-$	(62)
ΔyopE Yptb	*yopE-*	(82)
ΔyopH Yptb	*yopH-*	(85)
ΔyopM Yptb	*yopM-*	This study and (40)
ΔyopJ Yptb	*yopJ-*	(62)
ΔyopK Yptb	*yopK-*	(45)
ΔyopO Yptb	*yopO-*	(96)
ΔyopEH Yptb	*yopEH-*	(85)
ΔyopEK Yptb	*yopEK-*	This study and (97)
ΔyopHK Yptb	*yopHK-*	This study and (97)
ΔyopEHK Yptb	*yopEHK-*	This study and (97)

Figure s1 (related to Fig 1): *Yersinia* Yops suppress inflammasome activation. (A) Caco-2 cells were infected with PBS (Mock) or WT *Yptb* or *Δ6 Yptb*. Release of IL-1β into the supernatant was measured by ELISA at 6hpi. (B, C) Caco-2 cells were infected with PBS or WT *Yptb* or *Δ6 Yptb* at the indicated MOI. (B) Release of IL-18 into the supernatant was measured by ELISA at 6hpi. (C) Percent cytotoxicity normalized to cells treated with 2% triton were measured at 6hpi. * $p < 0.05$, ** $p < 0.01$ by one-way ANOVA. Error bars represent the standard deviation of triplicate wells and are representative of two independent experiments.

Figure s2 (related to Fig 2): Caspase-1 and caspase-8 are involved but not absolutely required for *Δ6 Yptb*-induced inflammasome activation in human IECs. (A) WT Caco-2 cells or two independent single cell clones of *CASP1*-/- Caco-2 cells were infected with PBS (Mock), WT *Yptb*, or *Δ6 Yptb*. (B) One hour prior to infection, WT Caco-2 cells were treated with 20 uM YVAD or DMSO as a vehicle control. Cells were then infected with PBS (Mock), WT *Yptb* or *Δ6 Yptb*. (A, B) IL-18 release into the supernatant was measured by ELISA at 6hpi. (C) Knockdown efficiency of siRNA targeting *CASP8* in WT Caco-2 cells was measured by qRT-PCR and normalized to housekeeping gene *HPRT* and calculated relative to control-siRNA-treated cells. (D) WT Caco-2 cells were treated with siRNA targeting a control scrambled siRNA or siRNA targeting *CASP8* for 72 hours. (E) One hour prior to infection WT Caco-2 cells were treated with 20 uM IETD or DMSO as a vehicle control. (D, E) Cells were infected with PBS (Mock), WT *Yptb* or *Δ6 Yptb*. IL-18 release into the supernatant was measured at 6hpi. (F-G) WT or two independent single cell clones of *CASP1*-/- Caco-2 cells were treated with siRNA targeting a control scrambled siRNA or siRNA targeting *CASP8* for 72 hours. (F) IL-18 release into the supernatant was measured at 6hpi. (G) Knockdown efficiency of siRNA targeting *CASP8* in WT Caco-2 cells was measured by qRT-PCR and normalized to housekeeping gene *HPRT* and calculated relative to control-siRNA-treated cells. ** $p < 0.01$, **** $p < 0.0001$ by two-way ANOVA. Error bars represent the standard deviation of triplicate wells and are representative of two or three independent experiments.

Figure s3 (related to Fig 2.): Caspase-5 contributes to *Δ6 Yptb*-induced inflammasome activation in human IECs (A) Knockdown efficiency of siRNA targeting *CASP5* in WT Caco-2 cells was measured by qRT-PCR, normalized to *HPRT* and calculated relative to control-siRNA-

698 treated cells. (B, C) WT Caco-2 cells were treated with siRNA targeting a control scrambled
699 siRNA or siRNA targeting *CASP5* for 72 hours. (B) IL-18 release and (C) % cytotoxicity
700 normalized to cells treated with 2% triton were measured at 6hpi. ** $p < 0.01$, **** $p < 0.0001$ by
701 two-way ANOVA. Error bars represent the standard deviation of triplicate wells and are
702 representative of three independent experiments.
703
704 Figure s4 (related to Fig 3.) NLRP3, NAIP/NLRC4 and ASC are dispensable for *Δ6 Yptb*-
705 induced inflammasome activation in human IECs. (A) One hour prior to infection cells were
706 treated with 10 uM MCC950 or DMSO as a vehicle control. Cells were then infected with PBS
707 (Mock) WT *Yptb* or *Δ6 Yptb.* (B, C) WT or two independent single cell clones of (B) *NAIP*-/- or
708 (C) *PYCARD*-/- Caco-2 cells were infected with PBS (Mock), WT *Yptb*, or *Δ6 Yptb*. (A, B, C) IL-
709 18 release was measured in supernatants at 6hpi. **** $p < 0.0001$ by two-way ANOVA. Error
710 bars represent the standard deviation of triplicate wells and are representative of three
711 independent experiments.
712
713 Figure s5 (related to Fig. 5): YopE and YopH block phagocytosis in human IECs. (A) WT Caco-
714 2 cells were infected with the indicated strain of *Yptb* at an MOI=20 and lysed at 2 hpi. Bacteria
715 were plated on *Yersinia*-selective agar to enumerate CFUs and %internalization was calculated
716 as 2hpi CFUs divided by bacterial inoculum. (B) WT Caco-2 cells were seeded on glass
717 coverslips and infected with indicated strain of *Yptb* expressing GFP at an MOI=20. Cells were
718 fixed at 2hpi and stained for extracellular *Yersinia* (Red) and DAPI to label DNA (blue). Number
719 of intracellular bacteria (green only) in a field and number of cells was scored by fluorescence
720 microscopy. Bars represent standard deviation of triplicate coverslips with 20 fields scored per
721 coverslip. (C) One hour prior to infection, WT Caco-2 cells were treated with 10 uM cytochalasin
722 D or DMSO as a vehicle control. Cells were then infected with PBS (Mock) or indicated strain of
723 *Yptb* and lysed at 2hpi. Bacteria were plated *Yersinia*-selective agar to enumerate CFUs
724 and %internalization was calculated as 2hpi CFUs divided by bacterial inoculum. * $p < 0.05$, ** p
725 < 0.01, **** $p < 0.0001$ by one-way ANOVA (A, B) or two-way ANOVA (C). Error bars represent
726 the standard deviation of triplicate wells and are representative of two or three independent
727 experiments.
728

1. Janeway CA. 1989. Approaching the Asymptote? Evolution and Revolution in Immunology. Cold Spring Harb Symp Quant Biol 54:1–13.
2. Janeway CA, Medzhitov R. 2003. Innate Immune Recognition. https://doi.org/101146/annurev.immunol20083001084359 20:197–216.
3. Vance RE, Isberg RR, Portnoy DA. 2009. Patterns of Pathogenesis: Discrimination of Pathogenic and Nonpathogenic Microbes by the Innate Immune System. Cell Host Microbe 6:10–21.
4. Brodsky IE, Monack D. 2009. NLR-mediated control of inflammasome assembly in the host response against bacterial pathogens. Semin Immunol 21:199–207.
5. Lamkanfi M, Dixit VM. 2009. Inflammasomes: guardians of cytosolic sanctity. Immunol Rev 227:95–105.
6. Mariathasan S, Weiss DS, Newton K, McBride J, O'Rourke K, Roose-Girma M, Lee WP, Weinrauch Y, Monack DM, Dixit VM. 2006. Cryopyrin activates the inflammasome in response to toxins and ATP. Nat 2006 4407081 440:228–232.
7. Muñoz-Planillo R, Kuffa P, Martínez-Colón G, Smith BL, Rajendiran TM, Núñez G. 2013. K+ Efflux Is the Common Trigger of NLRP3 Inflammasome Activation by Bacterial Toxins and Particulate Matter. Immunity 38:1142–1153.
8. Hornung V, Bauernfeind F, Halle A, Samstad EO, Kono H, Rock KL, Fitzgerald KA, Latz E. 2008. Silica crystals and aluminum salts activate the NALP3 inflammasome through phagosomal destabilization. Nat Immunol 2008 98 9:847–856.
9. Franchi L, Kanneganti TD, Dubyak GR, Núñez G. 2007. Differential requirement of P2X7 receptor and intracellular K+ for caspase-1 activation induced by intracellular and extracellular bacteria. J Biol Chem 282:18810–18818.
10. Ren T, Zamboni DS, Roy CR, Dietrich WF, Vance RE. 2006. Flagellin-Deficient Legionella Mutants Evade Caspase-1- and Naip5-Mediated Macrophage Immunity. PLOS Pathog 2:e18.
11. Zhao Y, Yang J, Shi J, Gong Y-N, Lu Q, Xu H, Liu L, Shao F. 2011. The NLRC4 inflammasome receptors for bacterial flagellin and type III secretion apparatus https://doi.org/10.1038/nature10510.
12. Kofoed EM, Vance RE. 2011. Innate immune recognition of bacterial ligands by NAIPs determines inflammasome specificity https://doi.org/10.1038/nature10394.
13. Miao EA, Mao DP, Yudkovsky N, Bonneau R, Lorang CG, Warren SE, Leaf IA, Aderem A. Innate immune detection of the type III secretion apparatus through the NLRC4 inflammasome https://doi.org/10.1073/pnas.0913087107.
14. Zhao Y, Shi J, Shi X, Wang Y, Wang F, Shao F. 2016. Genetic functions of the NAIP family of inflammasome receptors for bacterial ligands in mice. J Exp Med 213:647–656.
15. Rauch I, Tenthorey JL, Nichols RD, Al Moussawi K, Kang JJ, Kang C, Kazmierczak BI, Vance RE. 2016. NAIP proteins are required for cytosolic detection of specific bacterial ligands in vivo. J Exp Med 213:657–665.
16. Yang J, Zhao Y, Shi J, Shao F. 2013. Human NAIP and mouse NAIP1 recognize bacterial type III secretion needle protein for inflammasome activation. Proc Natl Acad Sci U S A 110:14408–14413.
17. Rayamajhi M, Zak DE, Chavarria-Smith J, Vance RE, Miao EA. 2013. Cutting Edge: Mouse NAIP1 Detects the Type III Secretion System Needle Protein. J Immunol 191:3986–3989.
18. Molofsky AB, Byrne BG, Whitfield NN, Madigan CA, Fuse ET, Tateda K, Swanson MS. 2006. Cytosolic recognition of flagellin by mouse macrophages restricts Legionella pneumophila infection. J Exp Med 203:1093–1104.
19. Shi J, Zhao Y, Wang K, Shi X, Wang Y, Huang H, Zhuang Y, Cai T, Wang F, Shao F. 2015. Cleavage of GSDMD by inflammatory caspases determines pyroptotic cell death. Nat 2015 5267575 526:660–665.

20. Li P, Allen H, Banerjee S, Franklin S, Herzog L, Johnston C, Mcdowell J, Paskind M, Rodman L, Salfeld J, Towne E, Tracey D, Wardwell S, Wei F-Y, Wong W, Kamen R, Seshadri T. 1995. Mice Deficient in IL-lp-Converting Enzyme Are Defective in Production of Mature IL-lp and Resistant to Endotoxic Shock. Cell 80:401–411.
21. Kuida K, Lippke JA, Ku G, Harding MW, Livingston DJ, Su MSS, Flavell RA. 1995. Altered Cytokine Export and Apoptosis in Mice Deficient in Interleukin-1β Converting Enzyme. Science (80-) 267:2000–2003.
22. Cookson BT, Brennan MA. 2001. Pro-inflammatory programmed cell death [2]. Trends Microbiol 9:113–114.
23. Mariathasan S, Monack DM. 2007. Inflammasome adaptors and sensors: intracellular regulators of infection and inflammation. Nat Rev Immunol 2007 71 7:31–40.
24. Kayagaki N, Warming S, Lamkanfi M, Walle L Vande, Louie S, Dong J, Newton K, Qu Y, Liu J, Heldens S, Zhang J, Lee WP, Roose-Girma M, Dixit VM. 2011. Non-canonical inflammasome activation targets caspase-11. Nature 479:117–121.
25. Kayagaki N, Stowe IB, Lee BL, O'Rourke K, Anderson K, Warming S, Cuellar T, Haley B, Roose-Girma M, Phung QT, Liu PS, Lill JR, Li H, Wu J, Kummerfeld S, Zhang J, Lee WP, Snipas SJ, Salvesen GS, Morris LX, Fitzgerald L, Zhang Y, Bertram EM, Goodnow CC, Dixit VM. 2015. Caspase-11 cleaves gasdermin D for non-canonical inflammasome signalling. Nat 2015 5267575 526:666–671.
26. Rathinam VAK, Vanaja SK, Waggoner L, Sokolovska A, Becker C, Stuart LM, Leong JM, Fitzgerald KA. 2012. TRIF licenses caspase-11-dependent NLRP3 inflammasome activation by gram-negative bacteria. Cell 150:606–619.
27. Gurung P, Subbarao Malireddi RK, Anand PK, Demon D, Vande Walle L, Liu Z, Vogel P, Lamkanfi M, Kanneganti TD. 2012. Toll or interleukin-1 receptor (TIR) domain-containing adaptor inducing interferon-β (TRIF)-mediated caspase-11 protease production integrates toll-like receptor 4 (TLR4) protein- and Nlrp3 inflammasome-mediated host defense against enteropathogens. J Biol Chem 287:34474–34483.
28. Broz P, Ruby T, Belhocine K, Bouley DM, Kayagaki N, Dixit VM, Monack DM. 2012. Caspase-11 increases susceptibility to Salmonella infection in the absence of caspase-1. Nat 2012 4907419 490:288–291.
29. Kayagaki N, Wong MT, Stowe IB, Ramani SR, Gonzalez LC, Akashi-Takamura S, Miyake K, Zhang J, Lee WP, Muszyński A, Forsberg LS, Carlson RW, Dixit VM. 2013. Noncanonical inflammasome activation by intracellular LPS independent of TLR4. Science 341:1246–1249.
30. Shi J, Zhao Y, Wang Y, Gao W, Ding J, Li P, Hu L, Shao F. 2014. Inflammatory caspases are innate immune receptors for intracellular LPS. Nature 514:187–192.
31. Hagar JA, Powell DA, Aachoui Y, Ernst RK, Miao EA. 2013. Cytoplasmic LPS activates caspase-11: implications in TLR4-independent endotoxic shock. Science 341:1250–1253.
32. Lamkanfi M, Dixit VM. 2014. Mechanisms and Functions of Inflammasomes. Cell 157:1013–1022.
33. Lamkanfi M, Dixit VM. 2010. Manipulation of Host Cell Death Pathways during Microbial Infections. Cell Host Microbe 8:44–54.
34. Labbé K, Saleh M. 2008. Cell death in the host response to infection. Cell Death Differ 2008 159 15:1339–1349.
35. Cornelis GR, Wolf-Watz H. 1997. The Yersinia Yop virulon: a bacterial system for subverting eukaryotic cells. Mol Microbiol 23:861–867.
36. Bliska JB, Wang X, Viboud GI, Brodsky IE. 2013. Modulation of innate immune responses by Yersinia type III secretion system translocators and effectors. Cell Microbiol 15:1622–1631.
37. Viboud GI, Bliska JB. 2005. YERSINIA OUTER PROTEINS: Role in Modulation of Host

Cell Signaling Responses and Pathogenesis. https://doi.org/101146/annurev.micro59030804121320 59:69–89.

38. Palmer LE, Hobble S, Galán JE, Bliska JB. 1998. YopJ of Yersinia pseudotuberculosis is required for the inhibition of macrophage TNF-α production and downregulation of the MAP kinases p38 and JNK. Mol Microbiol 27:953–965.
39. Orth K, Palmer LE, Bao ZQ, Stewart S, Rudolph AE, Bliska JB, Dixon JE. 1999. Inhibition of the Mitogen-Activated Protein Kinase Kinase Superfamily by a Yersinia Effector. Science (80-) 285:1920–1923.
40. Medici NP, Rashid M, Bliska JB. 2019. Characterization of pyrin dephosphorylation and inflammasome activation in macrophages as triggered by the Yersinia effectors YopE and YopT. Infect Immun 87.
41. Wang X, Parashar K, Sitaram A, Bliska JB. 2014. The GAP Activity of Type III Effector YopE Triggers Killing of Yersinia in Macrophages. PLoS Pathog 10:1004346.
42. Zwack EE, Feeley EM, Burton AR, Baofeng H, Yamamoto M, Kanneganti T-D, Bliska JB, Coers J, Brodsky IE. 2017. Guanylate Binding Proteins Regulate Inflammasome Activation in Response to. Infect Immun 85:1–16.
43. Zwack EE, Snyder AG, Wynosky-Dolfi MA, Ruthel G, Philip NH, Marketon MM, Francis MS, Bliska JB, Brodsky IE. 2015. Inflammasome activation in response to the yersinia type III secretion system requires hyperinjection of translocon proteins YopB and YopD. MBio 6:1–11.
44. Philip NH, Dillon CP, Snyder AG, Fitzgerald P, Wynosky-Dolfi MA, Zwack EE, Hu B, Fitzgerald L, Mauldin EA, Copenhaver AM, Shin S, Wei L, Parker M, Zhang J, Oberst A, Green DR, Brodsky IE. 2014. Caspase-8 mediates caspase-1 processing and innate immune defense in response to bacterial blockade of NF- B and MAPK signaling. Proc Natl Acad Sci 111:7385–7390.
45. Brodsky IE, Palm NW, Sadanand S, Ryndak MB, Sutterwala FS, Flavell RA, Bliska JB, Medzhitov R. 2010. A Yersinia effector protein promotes virulence by preventing inflammasome recognition of the type III secretion system. Cell Host Microbe 7:376–387.
46. Chung LK, Park YH, Zheng Y, Brodsky IE, Hearing P, Kastner DL, Chae JJ, Bliska JB. 2016. The Yersinia Virulence Factor YopM Hijacks Host Kinases to Inhibit Type III Effector-Triggered Activation of the Pyrin Inflammasome. Cell Host Microbe 20:296–306.
47. Lopes Fischer N, Naseer N, Shin S, Brodsky IE. 2020. Effector-triggered immunity and pathogen sensing in metazoans. Nat Microbiol 5:14–26.
48. Lei-Leston AC, Murphy AG, Maloy KJ. 2017. Epithelial Cell Inflammasomes in Intestinal Immunity and Inflammation. Front Immunol 8:1168.
49. Knodler LA, Crowley SM, Sham HP, Yang H, Wrande M, Ma C, Ernst RK, Steele-Mortimer O, Celli J, Vallance BA. 2014. Noncanonical inflammasome activation of caspase-4/caspase-11 mediates epithelial defenses against enteric bacterial pathogens. Cell Host Microbe 16:249–256.
50. Sellin ME, Müller AA, Felmy B, Dolowschiak T, Diard M, Tardivel A, Maslowski KM, Hardt WD. 2014. Epithelium-intrinsic NAIP/NLRC4 inflammasome drives infected enterocyte expulsion to restrict salmonella replication in the intestinal mucosa. Cell Host Microbe 16:237–248.
51. Hausmann A, Böck D, Geiser P, Berthold DL, Fattinger SA, Furter M, Bouman JA, Barthel-Scherrer M, Lang CM, Bakkeren E, Kolinko I, Diard M, Bumann D, Slack E, Regoes RR, Pilhofer M, Sellin ME, Hardt W-D. 2020. Intestinal epithelial NAIP/NLRC4 restricts systemic dissemination of the adapted pathogen Salmonella Typhimurium due to site-specific bacterial PAMP expression. Mucosal Immunol https://doi.org/10.1038/s41385-019-0247-0.
52. Rauch I, Deets KA, Ji DX, von Moltke J, Tenthorey JL, Lee AY, Philip NH, Ayres JS, Brodsky IE, Gronert K, Vance RE. 2017. NAIP-NLRC4 Inflammasomes Coordinate

Intestinal Epithelial Cell Expulsion with Eicosanoid and IL-18 Release via Activation of Caspase-1 and -8. Immunity 46:649–659.

53. Mitchell PS, Roncaioli JL, Turcotte EA, Goers L, Chavez RA, Lee AY, Lesser CF, Rauch I, Vance RE. 2020. Naip–nlrc4-deficient mice are susceptible to shigellosis. Elife 9:1–25.
54. Roncaioli JL, Babirye JP, Chavez RA, Liu FL, Turcotte EA, Lee AY, Lesser CF, Vance RE. 2022. A hierarchy of cell death pathways confers layered resistance to shigellosis in mice. bioRxiv 2022.09.21.508939.
55. Pallett MA, Crepin VF, Serafini N, Habibzay M, Kotik O, Sanchez-Garrido J, Di Santo JP, Shenoy AR, Berger CN, Frankel G. 2016. Bacterial virulence factor inhibits caspase-4/11 activation in intestinal epithelial cells. Mucosal Immunol 2017 103 10:602–612.
56. Naseer N, Zhang J, Bauer R, Constant DA, Nice TJ, Brodsky IE, Rauch I, Shin S. 2022. Salmonella enterica Serovar Typhimurium Induces NAIP/NLRC4- And NLRP3/ASC-Independent, Caspase-4-Dependent Inflammasome Activation in Human Intestinal Epithelial Cells. Infect Immun 90.
57. Kobayashi T, Ogawa M, Sanada T, Mimuro H, Kim M, Ashida H, Akakura R, Yoshida M, Kawalec M, Reichhart JM, Mizushima T, Sasakawa C. 2013. The Shigella OspC3 effector inhibits caspase-4, antagonizes inflammatory cell death, and promotes epithelial infection. Cell Host Microbe 13:570–583.
58. Ashida H, Mimuro H, Ogawa M, Kobayashi T, Sanada T, Kim M, Sasakawa C. 2011. Cell death and infection: A double-edged sword for host and pathogen survival. J Cell Biol 195:931–942.
59. Fink SL, Cookson BT. 2007. Pyroptosis and host cell death responses during Salmonella infection. Cell Microbiol 9:2562–2570.
60. Thinwa J, Segovia JA, Bose S, Dube PH. 2014. Integrin-Mediated First Signal for Inflammasome Activation in Intestinal Epithelial Cells. J Immunol 193:1373–1382.
61. Denecker G, Declercq W, Geuijen CAW, Boland A, Benabdillah R, Van Gurp M, Sory MP, Vandenabeele P, Cornelis GR. 2001. Yersinia enterocolitica YopP-induced apoptosis of macrophages involves the apoptotic signaling cascade upstream of bid. J Biol Chem 276:19706–19714.
62. Lilo S, Zheng Y, Bliska JB. 2008. Caspase-1 activation in macrophages infected with Yersinia pestis KIM requires the type III secretion system effector YopJ. Infect Immun 76:3911–3923.
63. Man SM, Hopkins LJ, Nugent E, Cox S, Glück IM, Tourlomousis P, Wright JA, Cicuta P, Monie TP, Bryant CE. 2014. Inflammasome activation causes dual recruitment of NLRC4 and NLRP3 to the same macromolecular complex. Proc Natl Acad Sci U S A 111:7403–7408.
64. Sarhan J, Liu BC, Muendlein HI, Li P, Nilson R, Tang AY, Rongvaux A, Bunnell SC, Shao F, Green DR, Poltorak A. 2018. Caspase-8 induces cleavage of gasdermin D to elicit pyroptosis during Yersinia infection. Proc Natl Acad Sci U S A 115:E10888–E10897.
65. Weng D, Marty-Roix R, Ganesan S, Proulx MK, Vladimer GI, Kaiser WJ, Mocarski ES, Pouliot K, Chan FKM, Kelliher MA, Harris PA, Bertin J, Gough PJ, Shayakhmetov DM, Goguen JD, Fitzgerald KA, Silverman N, Lien E. 2014. Caspase-8 and RIP kinases regulate bacteria-induced innate immune responses and cell death. Proc Natl Acad Sci U S A 111:7391–7396.
66. Antonopoulos C, Russo HM, El Sanadi C, Martin BN, Li X, Kaiser WJ, Mocarski ES, Dubyak GR. 2015. Caspase-8 as an Effector and Regulator of NLRP3 Inflammasome Signaling. J Biol Chem 290:20167–20184.
67. Agard NJ, Maltby D, Wells JA. 2010. Inflammatory stimuli regulate caspase substrate profiles. Mol Cell Proteomics 9:880–893.
68. He WT, Wan H, Hu L, Chen P, Wang X, Huang Z, Yang ZH, Zhong CQ, Han J. 2015. Gasdermin D is an executor of pyroptosis and required for interleukin-1β secretion. Cell

Res 2015 2512 25:1285–1298.
69. Liu X, Zhang Z, Ruan J, Pan Y, Magupalli VG, Wu H, Lieberman J. 2016. Inflammasome-activated gasdermin D causes pyroptosis by forming membrane pores. Nat 2016 5357610 535:153–158.
70. Sborgi L, Rühl S, Mulvihill E, Pipercevic J, Heilig R, Stahlberg H, Farady CJ, Müller DJ, Broz P, Hiller S. 2016. GSDMD membrane pore formation constitutes the mechanism of pyroptotic cell death. EMBO J 35:1766–1778.
71. Ding J, Wang K, Liu W, She Y, Sun Q, Shi J, Sun H, Wang DC, Shao F. 2016. Pore-forming activity and structural autoinhibition of the gasdermin family. Nat 2016 5357610 535:111–116.
72. Aglietti RA, Estevez A, Gupta A, Ramirez MG, Liu PS, Kayagaki N, Ciferri C, Dixit VM, Dueber EC. 2016. GsdmD p30 elicited by caspase-11 during pyroptosis forms pores in membranes. Proc Natl Acad Sci U S A 113:7858–7863.
73. Hu JJ, Liu X, Xia S, Zhang Z, Zhang Y, Zhao J, Ruan J, Luo X, Lou X, Bai Y, Wang J, Hollingsworth LR, Magupalli VG, Zhao L, Luo HR, Kim J, Lieberman J, Wu H. 2020. FDA-approved disulfiram inhibits pyroptosis by blocking gasdermin D pore formation. Nat Immunol 2020 217 21:736–745.
74. Valeria MRR, Ramirez J, Naseer N, Palacio NM, Siddarthan IJ, Yan BM, Boyer MA, Pensinger DA, Sauer JD, Shin S. 2017. Broad detection of bacterial type III secretion system and flagellin proteins by the human NAIP/NLRC4 inflammasome. Proc Natl Acad Sci U S A 114:13242–13247.
75. Naseer N, Egan MS, Reyes Ruiz VM, Scott WP, Hunter EN, Demissie T, Rauch I, Brodsky IE, Shin S. 2022. Human NAIP/NLRC4 and NLRP3 inflammasomes detect Salmonella type III secretion system activities to restrict intracellular bacterial replication. PLoS Pathog 18.
76. Gram AM, Wright JA, Pickering RJ, Lam NL, Booty LM, Webster SJ, Bryant CE. 2021. Salmonella Flagellin Activates NAIP/NLRC4 and Canonical NLRP3 Inflammasomes in Human Macrophages. J Immunol 206:631–640.
77. Dersch P, Isberg RR. 2000. An Immunoglobulin Superfamily-Like Domain Unique to the Yersinia pseudotuberculosis Invasin Protein Is Required for Stimulation of Bacterial Uptake via Integrin Receptors. Infect Immun 68:2930.
78. Isberg RR. 1989. Determinants for thermoinducible cell binding and plasmid-encoded cellular penetration detected in the absence of the Yersinia pseudotuberculosis invasin protein. Infect Immun 57:1998–2005.
79. Isberg RR, Tran Van Nhieu G. 1994. Binding and internalization of microorganisms by integrin receptors. Trends Microbiol 2:10–14.
80. Fallman M, Andersson K, Hakansson S, Magnusson KE, Stendahl O, Wolf- Watz H. 1995. Yersinia pseudotuberculosis inhibits Fc receptor-mediated phagocytosis in J774 cells. Infect Immun 63:3117–3124.
81. Andersson K, Carballeira N, Magnusson KE, Persson C, Stendahl O, Wolf-Watz H, Fällman M. 1996. YopH of Yersinia pseudotuberculosis interrupts early phosphotyrosine signalling associated with phagocytosis. Mol Microbiol 20:1057–1069.
82. Black DS, Bliska JB. 2000. The RhoGAP activity of the Yersinia pseudotuberculosis cytotoxin YopE is required for antiphagocytic function and virulence. Mol Microbiol 37:515–527.
83. Cornelis GR. 2002. The Yersinia Ysc–Yop “Type III” weaponry. Nat Rev Mol Cell Biol 2002 310 3:742–753.
84. Fasciano AC, Dasanayake GS, Estes MK, Zachos NC, Breault DT, Isberg RR, Tan S, Mecsas J. 2021. Yersinia pseudotuberculosis YopE prevents uptake by M cells and instigates M cell extrusion in human ileal enteroid-derived monolayers. Gut Microbes 13.
85. Black DS, Bliska JB. 1997. Identification of p130Cas as a substrate of Yersinia YopH

(Yop51), a bacterial protein tyrosine phosphatase that translocates into mammalian cells and targets focal adhesions. EMBO J 16:2730–2744.

86. Persson C, Carballeira N, Wolf-Watz H, Fällman M. 1997. The PTPase YopH inhibits uptake of Yersinia, tyrosine phosphorylation of p130Cas and FAK, and the associated accumulation of these proteins in peripheral focal adhesions. EMBO J 16:2307–2318.
87. Hamid N, Gustavsson A, Andersson K, McGee K, Persson C, Rudd CE, Fällman M. 1999. YopH dephosphorylates Cas and Fyn-binding protein in macrophages. Microb Pathog 27:231–242.
88. Zhen Y, Zhang H. 2019. NLRP3 inflammasome and inflammatory bowel disease. Front Immunol 10:276.
89. Holly MK, Han X, Zhao EJ, Crowley SM, Allaire JM, Knodler LA, Vallance BA, Smith JG. 2020. Salmonella enterica infection of murine and human enteroid-derived monolayers elicits differential activation of epithelium-intrinsic inflammasomes. Infect Immun 88.
90. Mills SD, Finlayl BB. 1998. Isolation and characterization of Salmonella typhimurium and Yersinia pseudotubercu/osis-containing phagosomes from infected mouse macrophages: Y; pseudotuberculosis traffics to terminal lysosomes where they are degraded. Eur J Cell Biol 77:35–47.
91. Fallman M, Andersson K, Hakansson S, Magnusson KE, Stendahl O, Wolf- Watz H. 1995. Yersinia pseudotuberculosis inhibits Fc receptor-mediated phagocytosis in J774 cells. Infect Immun 63:3117–3124.
92. Feeley EM, Pilla-Moffett DM, Zwack EE, Piro AS, Finethy R, Kolb JP, Martinez J, Brodsky IE, Coers J. 2017. Galectin-3 directs antimicrobial guanylate binding proteins to vacuoles furnished with bacterial secretion systems. Proc Natl Acad Sci U S A 114:E1698–E1706.
93. Ventayol PS, Geiser P, Di Martino ML, Florbrant A, Fattinger SA, Walder N, Sima E, Shao F, Gekara NO, Sundbom M, Hardt WD, Webb DL, Hellström PM, Eriksson J, Sellin ME. 2021. Bacterial detection by NAIP/NLRC4 elicits prompt contractions of intestinal epithelial cell layers. Proc Natl Acad Sci U S A 118:1–11.
94. Zhang Y, Murtha J, Roberts MA, Siegel RM, Bliska JB. 2008. Type III secretion decreases bacterial and host survival following phagocytosis of Yersinia pseudotuberculosis by macrophages. Infect Immun 76:4299–4310.
95. Livak KJ, Schmittgen TD. 2001. Analysis of Relative Gene Expression Data Using Real-Time Quantitative PCR and the 2−ΔΔCT Method. Methods 25:402–408.
96. Viboud GI, So SSK, Ryndak MB, Bliska JB. 2003. Proinflammatory signalling stimulated by the type III translocation factor YopB is counteracted by multiple effectors in epithelial cells infected with Yersinia pseudotuberculosis. Mol Microbiol 47:1305–1315.
97. Ryndak MB, Chung H, London E, Bliska JB. 2005. Role of predicted transmembrane domains for Type III translocation, pore formation, and signaling by the Yersinia pseudotuberculosis YopB protein. Infect Immun 73:2433–2443.

Figure 1

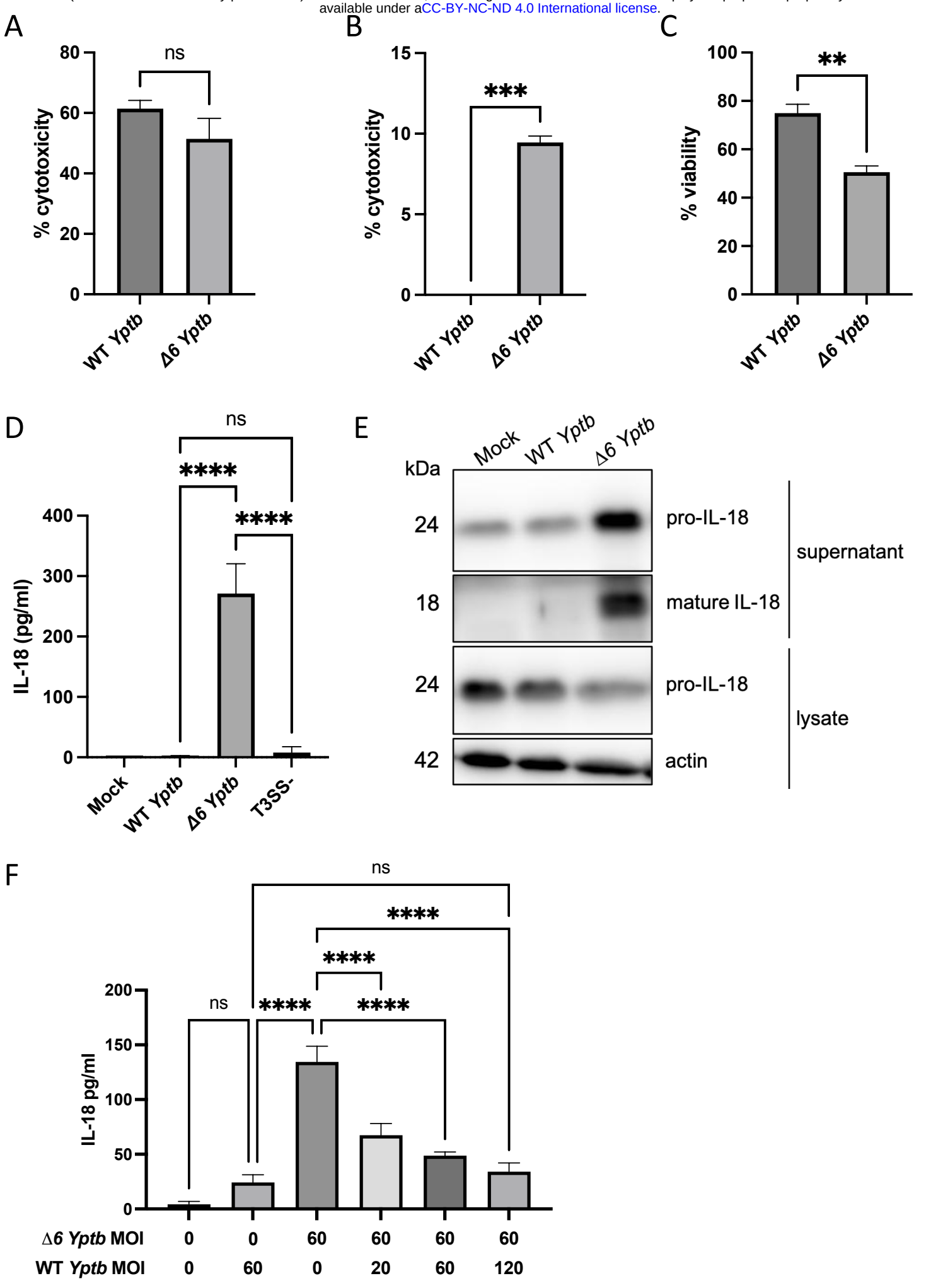

Figure 2

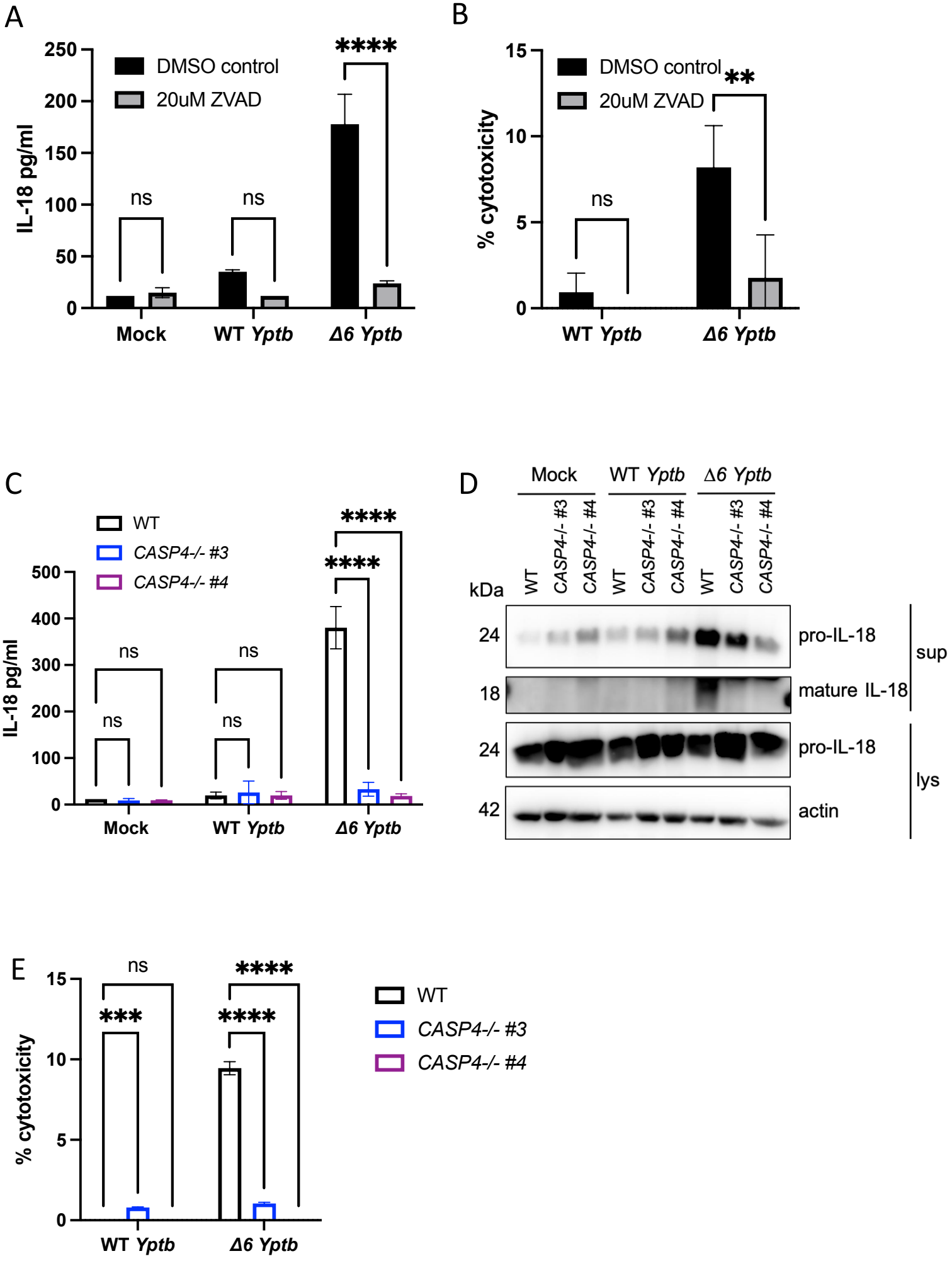

Figure 3

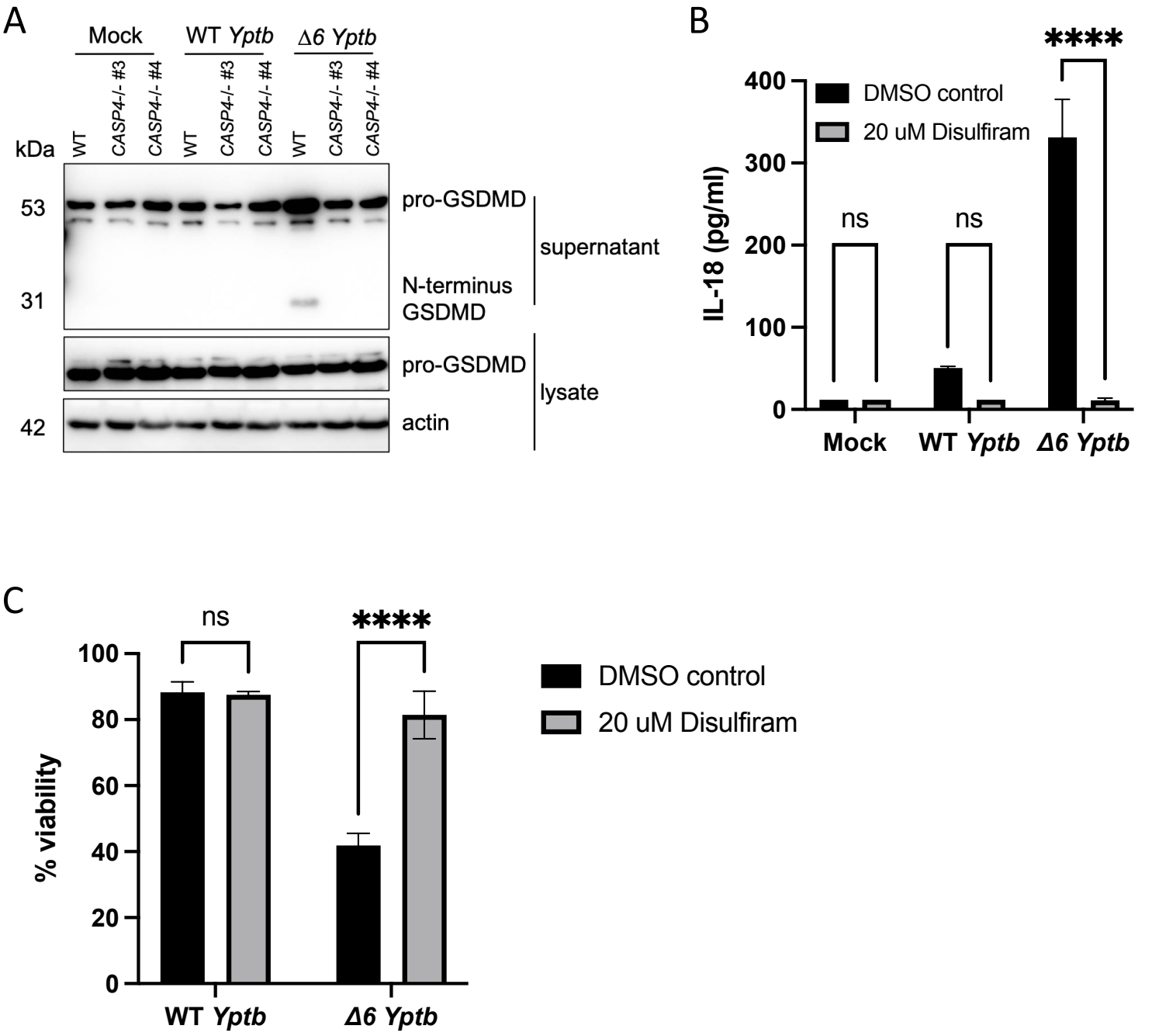

Figure 4

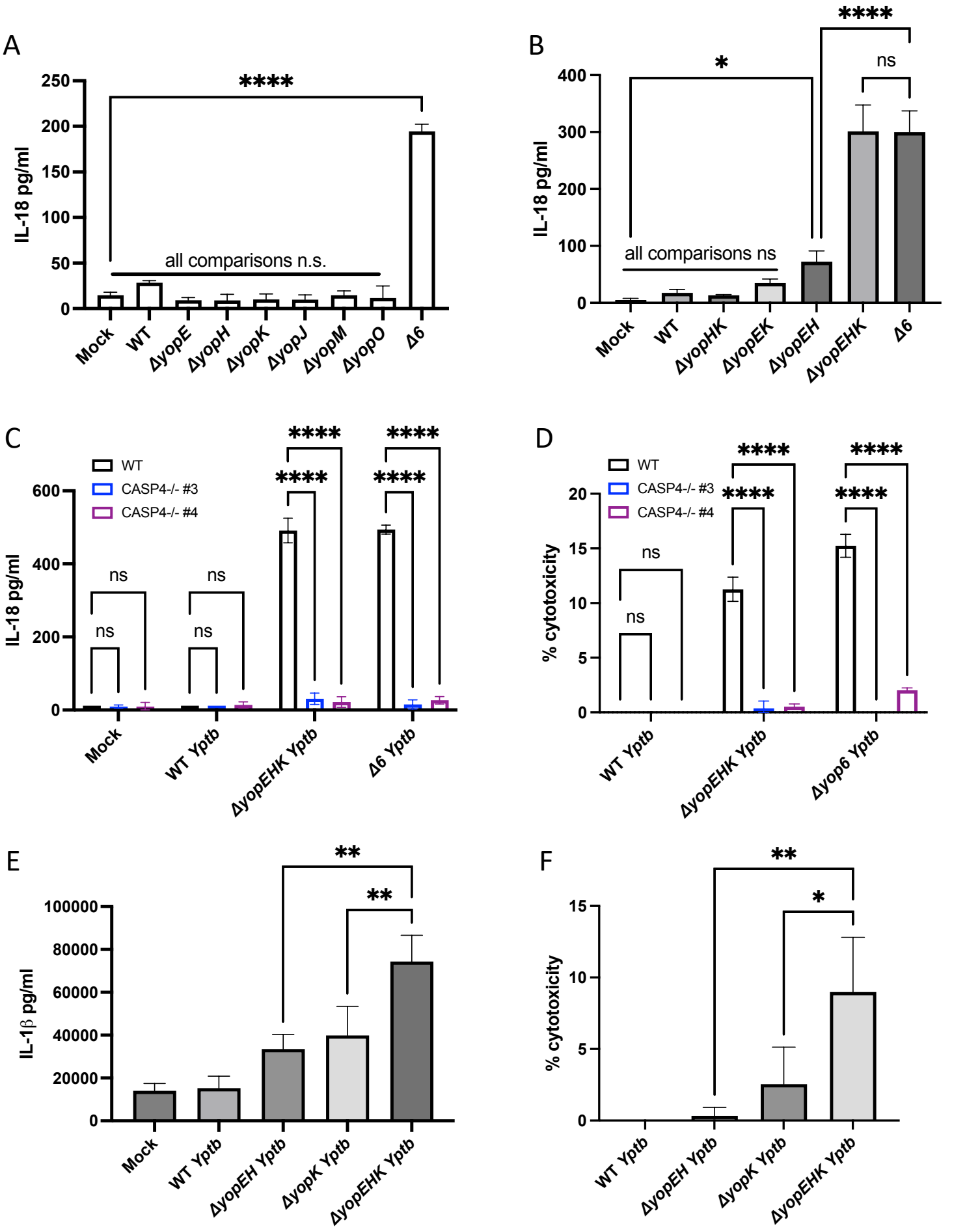

Figure 5

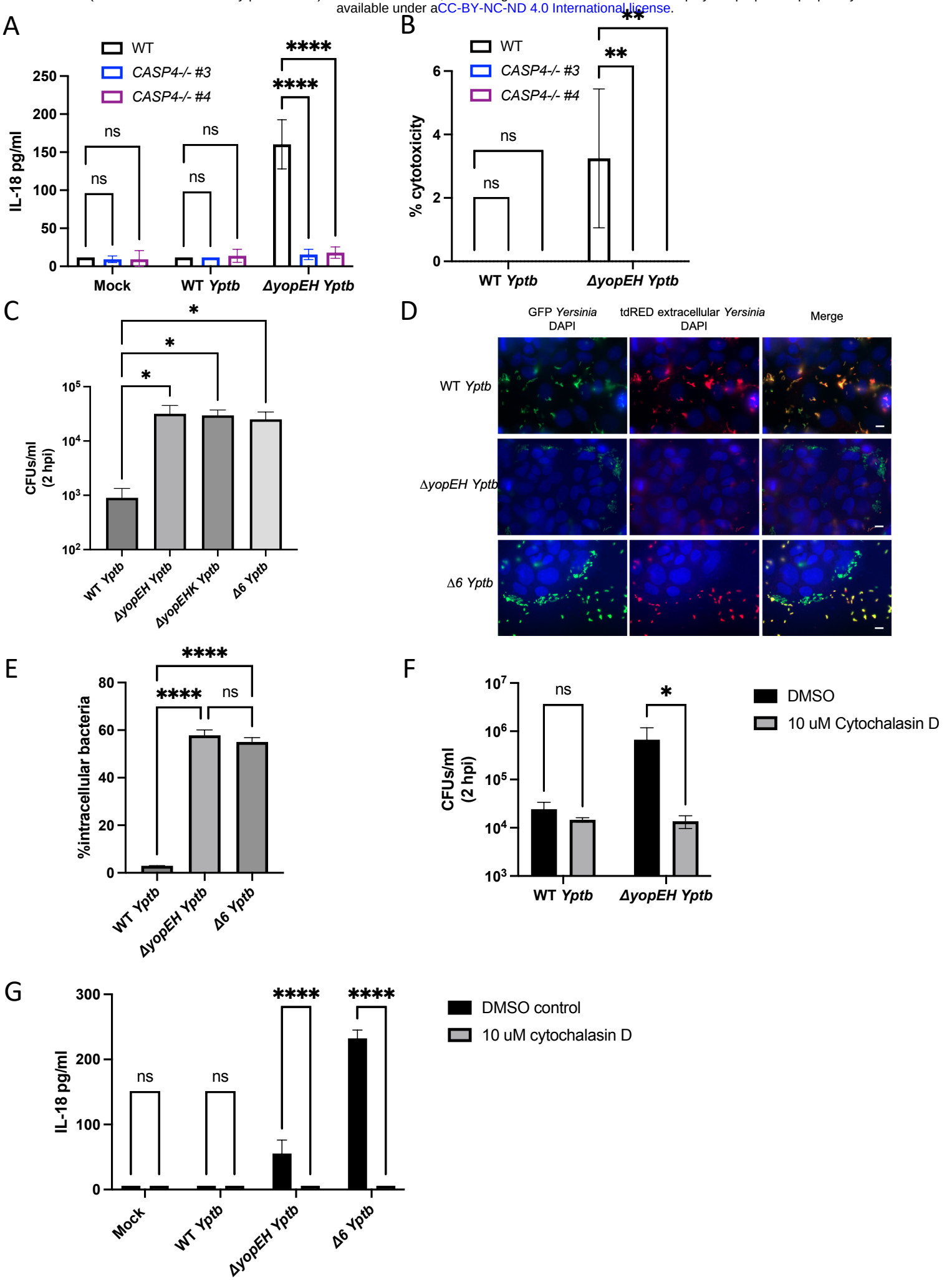

Figure S1

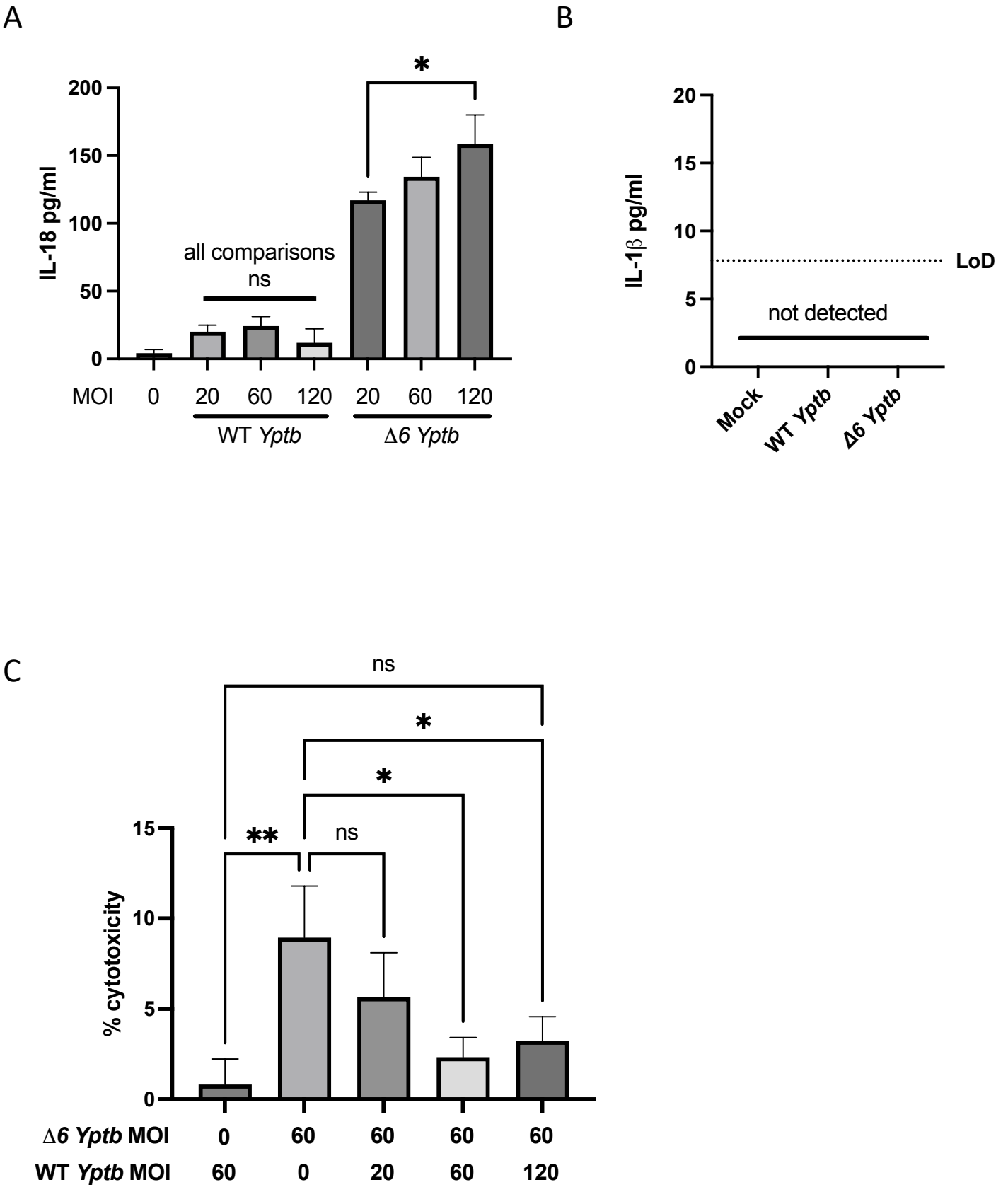

Figure S2

A

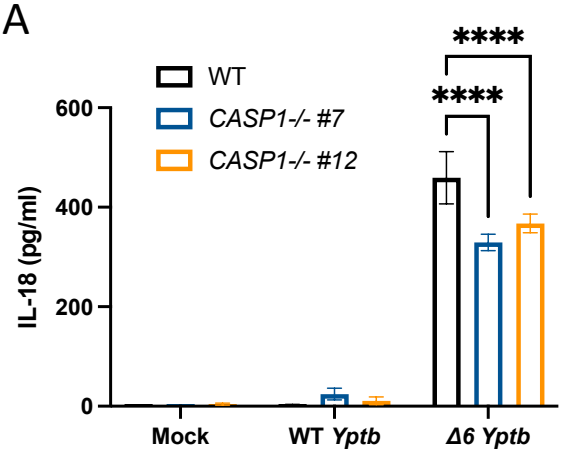

B

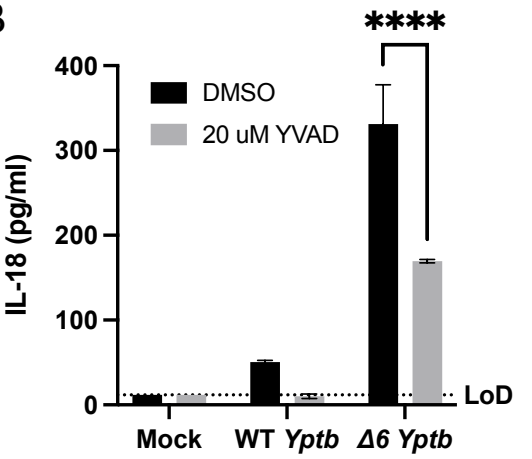

C

Average knockdown efficiency

	CASP8
WT	72%

D

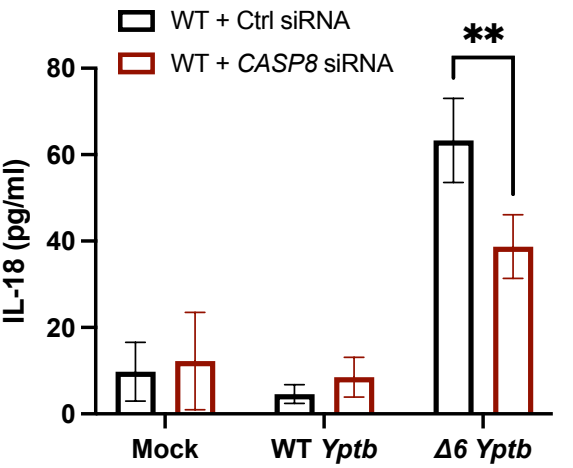

E

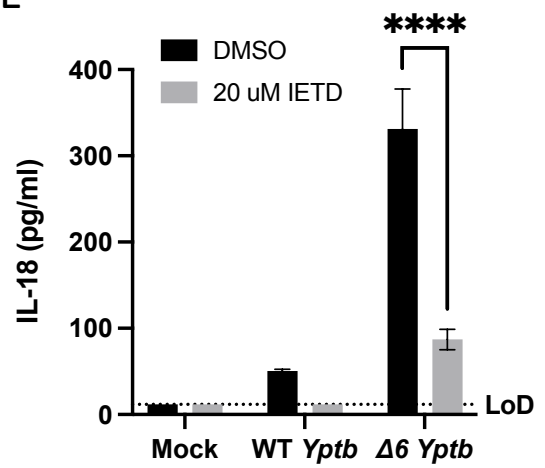

F

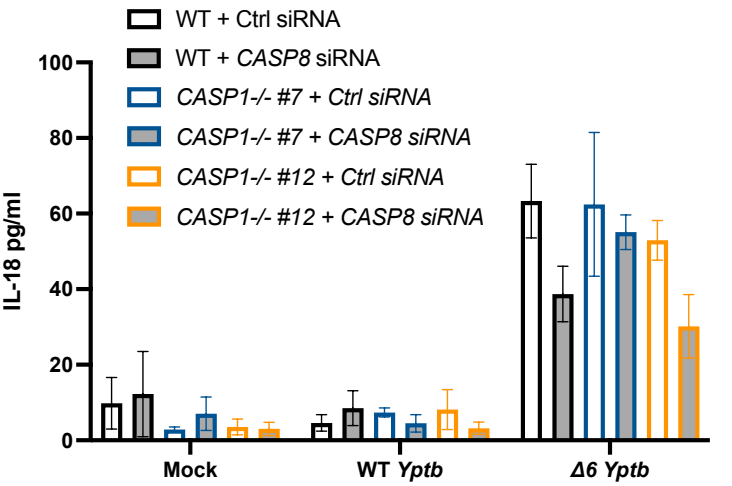

S2G

Average knockdown efficiency

	CASP8
WT	57%
CASP1-/- #7	68%
CASP1-/- #12	74%

Figure S3

A

Average knockdown efficiency

	CASP5
WT Caco-2s	75%

B

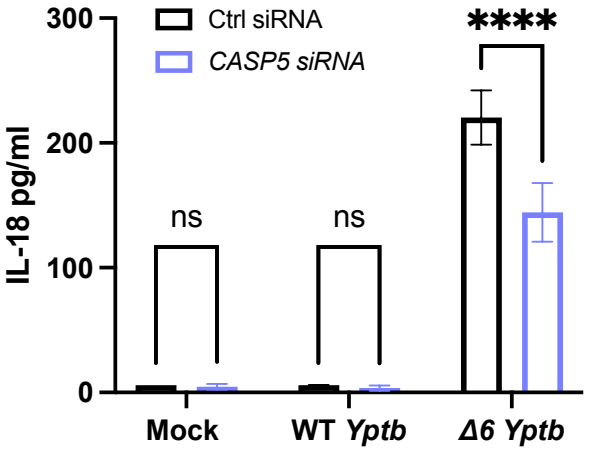

C

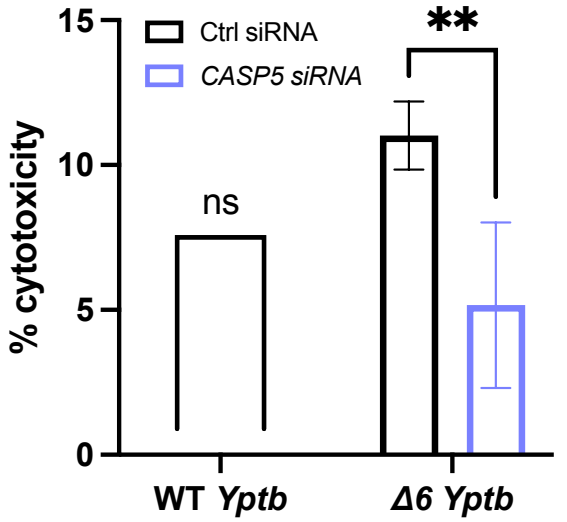

Figure S4

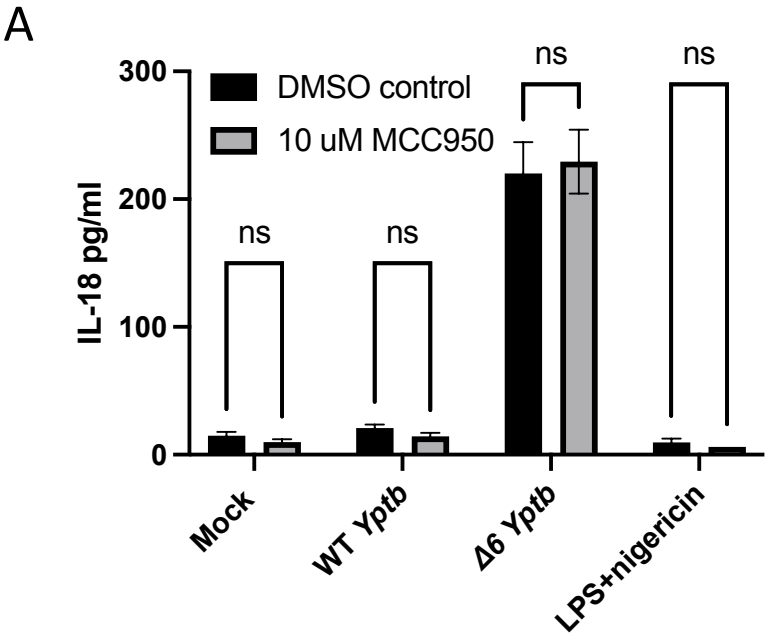

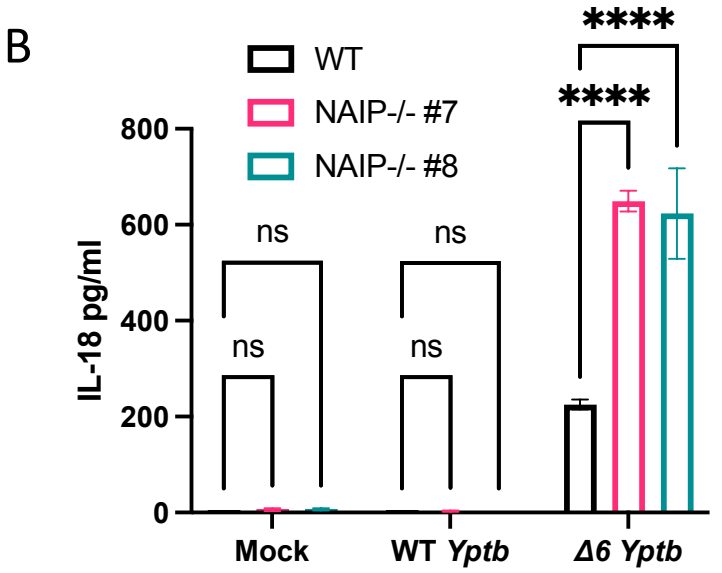

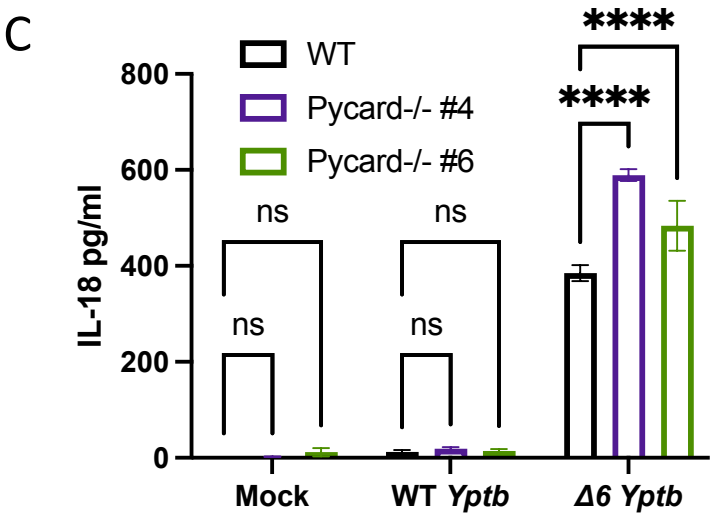

Figure S5